



# Deep Phenotyping by Mass Cytometry and Single-Cell RNA-Sequencing Reveals LYN-Regulated Signaling Profiles Underlying Monocyte Subset Heterogeneity and Lifespan

Morgan E. Roberts,\* Maunish Barvalia,\* Jessica A.F.D. Silva, Rachel A. Cederberg, William Chu, Amanda Wong, Daven C. Tai, Sam Chen, Israel Matos, John J. Priatel, Pieter R. Cullis, Kenneth W. Harder

**RATIONALE:** Monocytes are key effectors of the mononuclear phagocyte system, playing critical roles in regulating tissue homeostasis and coordinating inflammatory reactions, including those involved in chronic inflammatory diseases such as atherosclerosis. Monocytes have traditionally been divided into 2 major subsets termed conventional monocytes and patrolling monocytes (pMo) but recent systems immunology approaches have identified marked heterogeneity within these cells, and much of what regulates monocyte population homeostasis remains unknown. We and others have previously identified LYN tyrosine kinase as a key negative regulator of myeloid cell biology; however, LYN's role in regulating specific monocyte subset homeostasis has not been investigated.

**OBJECTIVE:** We sought to comprehensively profile monocytes to elucidate the underlying heterogeneity within monocytes and dissect how *Lyn* deficiency affects monocyte subset composition, signaling, and gene expression. We further tested the biological significance of these findings in a model of atherosclerosis.

**METHODS AND RESULTS:** Mass cytometric analysis of monocyte subsets and signaling pathway activation patterns in conventional monocytes and pMos revealed distinct baseline signaling profiles and far greater heterogeneity than previously described. *Lyn* deficiency led to a selective expansion of pMos and alterations in specific signaling pathways within these cells, revealing a critical role for LYN in pMo physiology. LYN's role in regulating pMos was cell-intrinsic and correlated with an increased circulating half-life of *Lyn*-deficient pMos. Furthermore, single-cell RNA sequencing revealed marked perturbations in the gene expression profiles of *Lyn*<sup>-/-</sup> monocytes with upregulation of genes involved in pMo development, survival, and function. *Lyn* deficiency also led to a significant increase in aorta-associated pMos and protected *Ldlr*<sup>-/-</sup> mice from high-fat diet-induced atherosclerosis.

**CONCLUSIONS:** Together our data identify LYN as a key regulator of pMo development and a potential therapeutic target in inflammatory diseases regulated by pMos.

**VISUAL OVERVIEW:** An online [visual overview](#) is available for this article.

**Key Words:** atherosclerosis ■ homeostasis ■ monocytes ■ signal transduction ■ transcriptome

**Editorial, see p 1324 | In This Issue, see p 1321 | Meet the First Author, see p 1322**

**M**onocytes are important members of the mononuclear phagocyte system that contribute to tissue homeostasis, inflammation, and resolution of inflammatory responses.<sup>1,2</sup> They are predominantly

circulatory cells comprising ≈10% of murine blood leukocytes but also residing in bone marrow (BM) and spleen.<sup>3–5</sup> Monocytes are heterogeneous, but can be identified by expression of CD11b and CSF-1R (colony-stimulating

Correspondence to: Kenneth W. Harder, PhD, Department of Microbiology and Immunology, Life Sciences Institute, University of British Columbia, 2350 Health Sciences Mall, Vancouver, British Columbia, Canada. Email [ken.harder@ubc.ca](mailto:ken.harder@ubc.ca)

\*M.E.R. and M.B. contributed equally to this article.

The Data Supplement is available with this article at <https://www.ahajournals.org/doi/suppl/10.1161/CIRCRESAHA.119.315708>.

For Sources of Funding and Disclosures, see page e77.

© 2020 American Heart Association, Inc.

Circulation Research is available at [www.ahajournals.org/journal/res](http://www.ahajournals.org/journal/res)

Novelty and Significance

What Is Known?

- Monocytes are divided into 2 major subsets, conventional/classical monocytes and patrolling/nonclassical monocytes (pMos), which have distinct functions.
- LYN is a key regulator of myeloid cells, playing dual, activating, and inhibitory roles.

What New Information Does This Article Contribute?

- Identifies marked heterogeneity within monocytes with respect to surface marker expression and baseline signaling profiles.
- Establishes that within monocytes, LYN is a key regulator of pMos signaling and lifespan.
- Demonstrates that *Lyn* deficiency confers protection from high-fat diet–induced atherosclerosis.

Monocytes are comprised of 2 major subsets; conventional/classical monocytes extravasate into tissues and are precursors of some macrophages, whereas

pMos remain in the vasculature and play a crucial role in maintaining the vascular integrity of the endothelium. LYN is a Src-family tyrosine kinase which acts as a dual, context dependent positive or negative regulator in various myeloid cells; however, LYN's precise role in monocyte subsets is not known. Here, we show that within monocytes, LYN selectively acts as a negative regulator of pMos. *Lyn* deficiency causes an expansion of pMos in circulation and further increases their lifespan. Using systems immunology approaches such as mass cytometry and single cell RNA-sequencing we show that *Lyn* deficiency causes marked changes to the surface marker expression and signaling profiles of monocytes, and an expansion of specific clusters of pMos, and increases the expression of genes crucial in pMo development. Lastly, with *Lyn* deficiency, we also see a selective expansion of aorta-associated pMos and diminished high-fat diet–induced atherosclerosis.

Nonstandard Abbreviations and Acronyms

<b>BM</b>	bone marrow
<b>BM-Mo</b>	bone marrow-derived monocyte
<b>cMo</b>	conventional monocyte
<b>cMoP</b>	common monocyte progenitor
<b>CSF-1R</b>	colony-stimulating factor-1 receptor, CD115
<b>CyTOF</b>	mass cytometry
<b>intMo</b>	intermediate monocyte
<b>pMo</b>	patrolling monocyte
<b>pTyr</b>	phospho tyrosine
<b>oxLDL</b>	oxidized low-density lipoprotein
<b>SFK</b>	Src family of tyrosine kinases
<b>wt</b>	wildtype

factor-1 receptor; CD115). Murine monocytes are generally classified into 2 main subsets, conventional monocytes (cMo) which express Ly6C (lymphocyte antigen 6 complex, locus C), and nonconventional or patrolling monocytes (pMo) which lack Ly6C expression.<sup>6</sup> cMos are also distinguished based on expression of CD62L (L-selectin) and CCR2 (C-C chemokine receptor type 2), whereas pMos lack these markers and express CD43, CD11c, CD274, and FcγRIV (low-affinity immunoglobulin gamma Fc region receptor IV).<sup>7–9</sup> Recent transcriptomic, epigenomic, and fate-mapping studies have refined the developmental trajectory of monocytes, supporting the

notion that cMos are the obligate precursors of pMos that gradually transition into pMos via a Ly6C<sup>int</sup>FcγRIV<sup>int</sup> population termed intermediate monocytes (intMo).<sup>5,10–12</sup> Hence, monocytes are a heterogeneous group of cells broadly categorized into cMos, pMos, and intMos. Human equivalents have been identified and can be distinguished by differential expression CD14 and CD16, with cMos being CD14<sup>hi</sup>CD16<sup>–</sup>, intMos being CD14<sup>hi</sup>CD16<sup>+</sup> and pMos being CD14<sup>lo</sup>CD16<sup>+</sup>.<sup>13,14</sup>

All 3 monocyte subsets can extravasate into tissues during infection or inflammation where they can differentiate into a variety of effector cells with inflammatory and antigen presentation capabilities depending on environmental cues.<sup>2,6,7,10,15–19</sup> Steady-state pMos patrol the vasculature where they scavenge particles such as lipoproteins, protein aggregates, and necrotic cells, and survey and maintain endothelial integrity.<sup>14,20–22</sup> As such, pMos may play a role in preventing diseases such as atherosclerosis<sup>23,24</sup> and Alzheimer disease.<sup>21</sup> There is also evidence that pMos antagonize tumour metastasis to the lung.<sup>25–27</sup> However, a pathogenic role for pMos has been suggested in arthritis<sup>28</sup> and systemic lupus erythematosus,<sup>29–31</sup> and pMos have been implicated in resistance to anti-VEGFR2 (vascular endothelial growth factor receptor 2) therapy in colorectal cancer.<sup>32</sup>

Little is known about how pMo development and homeostasis are regulated; however, the transcription factors NR4A1 (nuclear receptor subfamily 4 group A member 1; Nur77) and C/EBPβ (CCAAT enhancer-binding protein beta) were identified as master regulators of pMo differentiation and survival.<sup>8,11,12,33</sup> Further studies

identified CX<sub>3</sub>CR1 (C-X<sub>3</sub>-C motif chemokine receptor 1) as a pMo survival factor,<sup>34</sup> and sphingosine-1-phosphate receptor signaling is required for pMo egress from BM and spleen.<sup>35,36</sup> The circulating lifespan of pMos can also be dynamically regulated, in part through CSF-1R signaling.<sup>5,33</sup> Alterations in monocyte homeostasis can impact proinflammatory responses as well as the resolution of inflammation and tissue repair. Monocytes are particularly important in the development and progression of atherosclerosis, a chronic inflammatory disease resulting from altered lipid metabolism and inappropriate vessel immune responses.<sup>37–39</sup> Although the role of pMos in atherosclerosis is still poorly defined, pMos can take up oxidized lipoproteins,<sup>40</sup> and pMo-deficient *Nr4a1*<sup>−/−</sup> mice develop exacerbated atherosclerosis,<sup>23,24</sup> suggesting a protective role for these cells. Given the importance of monocytes in cardiovascular and other chronic inflammatory diseases, it is critical to better understand the factors that regulate their homeostasis and functions.

LYN (Lck/yes novel tyrosine kinase) is a member of the Src family of tyrosine kinases (SFK) that is expressed throughout the hematopoietic system, except T cells and some innate lymphoid cells,<sup>41,42</sup> and in nonhematopoietic cells such as epithelial cells.<sup>43–45</sup> In mononuclear phagocytes, LYN is an important negative regulator of signaling downstream of receptors involved in cell survival, proliferation, and adhesion.<sup>46</sup> We have previously shown that *Lyn* deficiency results in an age-dependent expansion of myeloid cells, including monocytes, that leads to the development of myeloproliferative disease.<sup>47</sup> This includes increased myeloid cells in blood, BM, and spleen and an increase in myeloid progenitors in spleens of aged *Lyn*<sup>−/−</sup> mice.<sup>47–49</sup>

Although LYN is known to be a critical regulator of mononuclear phagocyte development and function, much of the work was done before the identification of biologically distinct monocyte subsets; therefore, LYN's role in monocyte subsets has not been explored. Here, we show that LYN is a key regulator of monocyte subset development and circulating lifespan. Loss of LYN resulted in pMo accumulation with age, which was independent of the adaptive immune system. LYN's ability to regulate pMo populations was cell-intrinsic and not due to accumulation of BM progenitors but correlated with increased splenic monocyte progenitors. Loss of LYN resulted in increased BM-derived monocyte survival in vitro and increased circulating pMo half-life in vivo. Interrogation of monocyte subset composition and signaling at high resolution using mass cytometry (CyTOF) revealed distinct monocyte subsets and signal transduction pathway patterns underlying cMo and pMo heterogeneity, with loss of LYN associated with failure to establish normal levels of tyrosine phosphorylation and other signaling patterns associated with development of pMos from cMos. Using single-cell RNA-sequencing, we comprehensively profiled the transcriptomic landscape of wildtype (wt) and

*Lyn*-deficient monocytes. We found an upregulation of various pMo defining genes in *Lyn*-deficient cMos and pMos compared with their wt counterparts. Finally, *Lyn* deficiency in innate immune cells was associated with diminished atherosclerosis correlating with increased circulatory and vessel-associated pMos. Thus, we show that LYN is a key regulator of monocyte subset composition and signaling pathways governing pMo number and lifespan, and that distinct signaling profiles distinguish cMos and pMos.

## METHODS

Materials and methods are included in the [Data Supplement](#).

The monocyte single cell RNA-seq data is deposited in NCBI GEO and can be accessed using the accession id: GSE146216, and the R analysis script from the Github repository of Maunish Barvalia at [https://github.com/maunishb/harder\\_lab\\_analysis](https://github.com/maunishb/harder_lab_analysis). All the other data and materials that support the findings of this study are available from the corresponding author upon reasonable request.

## RESULTS

### LYN Negatively Regulates pMo Populations

To identify novel roles for LYN as a regulator of the immune system, we compared steady-state differences in wt and *Lyn*<sup>−/−</sup> mouse blood leukocytes by CyTOF using a panel of 37 antibodies (Table 1 in the [Data Supplement](#)). A t-distributed stochastic neighbor embedding algorithm and its visualization tool was used for dimensionality reduction and clustering.<sup>50</sup> This systems-level assessment of blood cell composition confirmed previous studies showing significantly decreased B cell frequency, especially mature and CD150<sup>+</sup> B cells, and increased total monocytes in *Lyn*<sup>−/−</sup> mice (Figure 1A).<sup>46–48,51</sup> Monocytes clustered into 4 subsets: cMos, pMos, and 2 intMos clusters that differed in MHCII (major histocompatibility complex class II) expression (Figure 1B). The frequencies of all monocyte subsets within total white blood cells were increased in *Lyn*<sup>−/−</sup> mice, with pMos showing the greatest increase (Figure 1A).

We next used flow cytometry to further investigate LYN's role in regulating steady-state monocyte populations. Given the age-dependent development of myeloproliferative disease in *Lyn*<sup>−/−</sup> mice,<sup>46–48</sup> we examined the monocyte compartment of young (8–10 weeks) and aged (26–30 weeks) wt and *Lyn*<sup>−/−</sup> mice. Blood, BM, and spleen were harvested from naïve mice, and monocyte subsets were identified based on expression of CD11b, CD115, Ly6C, CD62L, and CD11c (Figure 1A in the [Data Supplement](#)). Both young and aged *Lyn*<sup>−/−</sup> mice had a significantly increased frequency (≈2-fold and 4-fold) and number (≈1.5-fold and 3-fold) of total blood monocytes compared with wt mice, which increased with age



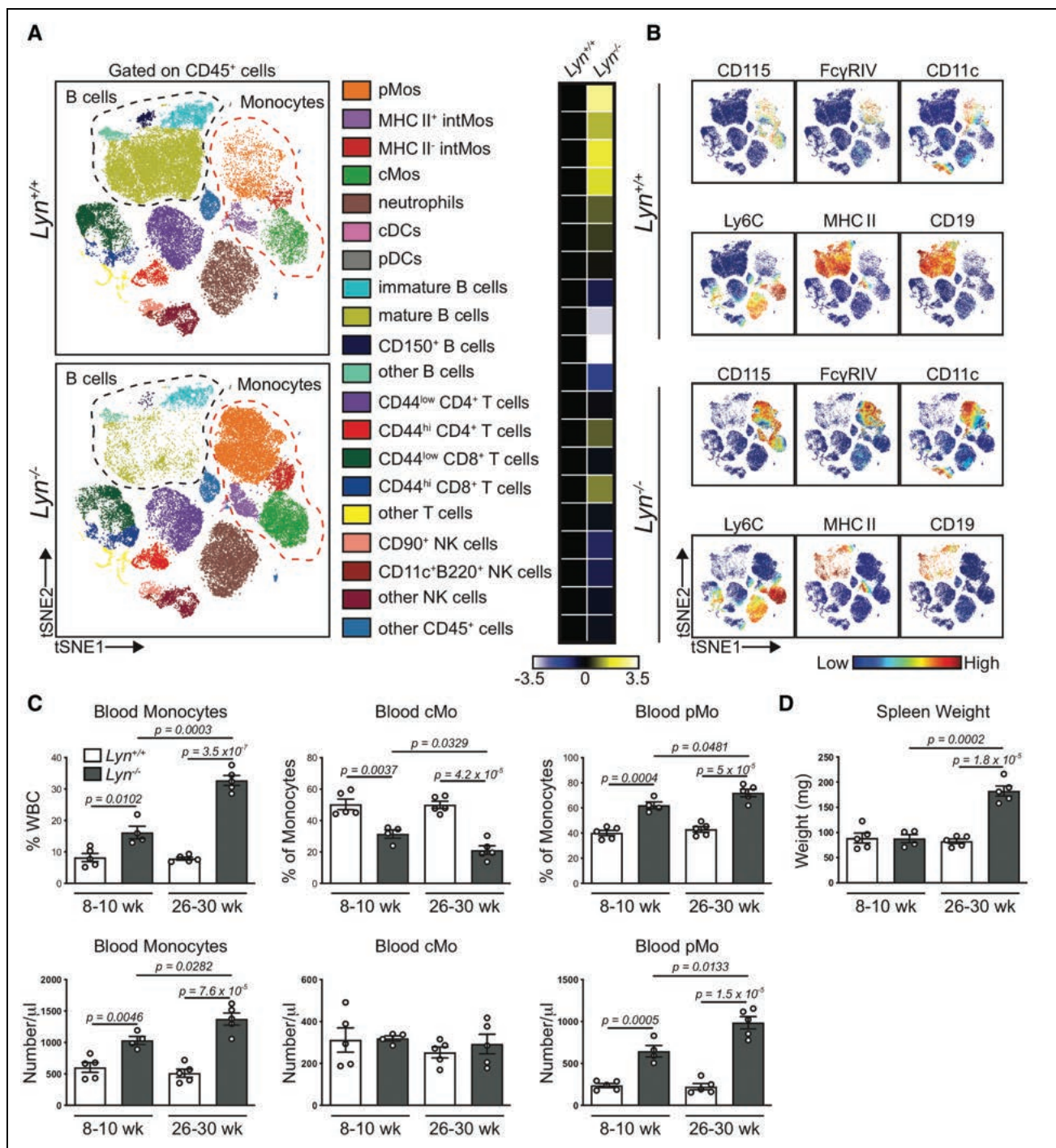


**Figure 1. LYN regulates circulating patrolling monocyte numbers.**

**A** and **B**, Blood was collected from naive *Lyn*<sup>+/+</sup> (*n*=5, pooled) and *Lyn*<sup>-/-</sup> (*n*=5, pooled) mice and cells and analyzed by mass cytometry (CyTOF) using a panel of 37 antibodies. **A**, t-distributed stochastic neighbor embedding algorithm (t-SNE) analysis was performed on CD45<sup>+</sup> cells and the indicated immune cell subsets were identified by manual gating. Black dotted line indicates B cell subsets and red dotted line indicates monocyte subsets. Log2 normalized relative frequency (% white blood cell [WBC]) was used to generate the heatmap. **B**, viSNE plots are colored according to the expression of the indicated markers. **C**, Blood was collected from young (8–10 wk) and aged (26–30 wk) naive *Lyn*<sup>+/+</sup> and *Lyn*<sup>-/-</sup> mice, and monocyte populations were assessed by flow cytometry. **Top**, Frequency of monocytes (as % WBC) and monocyte subsets (as % of total monocytes) are shown. **Bottom**, Numbers of total blood monocytes, conventional monocytes (cMo), and patrolling monocytes (pMo) are enumerated. **D**, Spleen weights from the mice are shown. Representative data from at least 3-independent experiments are shown, *n*=4–5/group. Statistical significance was assessed using an unpaired Student *t* test. Data are mean±SEM. cDC indicates conventional dendritic cell; FcγRIV, low-affinity immunoglobulin gamma Fc region receptor IV; MHC II, major histocompatibility complex class II; NK, natural killer; and pDC, plasmacytoid dendritic cell.

(Figure 1C). This was independent of overt myeloproliferative disease as it occurred before development of splenomegaly in *Lyn*<sup>-/-</sup> mice (Figure 1D). *Lyn*<sup>-/-</sup> mice also exhibited an increased frequency of monocytes in BM and spleen (Figure 1B and 1C in the [Data Supplement](#)) and increased total number of monocytes in spleen that was significantly higher in aged mice (Figure 1E in the [Data Supplement](#)).

The monocyte compartment was skewed towards pMos in *Lyn*<sup>-/-</sup> mice in all tissues examined, with an increased frequency of pMos and decreased frequency of cMos within total monocytes (Figure 1C and Figure 1B and 1C in the [Data Supplement](#)). Analysis of cell numbers indicated that loss of LYN did not impact cMo populations (Figure 1C and Figure 1D and 1E in the [Data Supplement](#)). Instead, *Lyn* deficiency resulted in significant expansion of pMos in blood, BM, and spleen, in young and aged *Lyn*<sup>-/-</sup> mice. Importantly, LYN's role in regulating pMos was independent of the adaptive immune system, as *Lyn* deficiency in *Rag1*<sup>-/-</sup> mice, which lack mature T and B cells<sup>52</sup> (Figure 1IA in the [Data Supplement](#)), led to a significant increase in pMos in blood,

BM, and spleen with no effect on cMo numbers (Figure 1I in the [Data Supplement](#)). Since a more moderate decrease in *Lyn* activity may have more relevance to human disease, we assessed the effect of loss of a single *Lyn* allele (*Lyn*<sup>+/-</sup>) on monocyte populations. *Lyn*<sup>+/-</sup> mice had an increase in frequency and number of pMos in blood but not BM compared with wt controls (Figure 1II in the [Data Supplement](#)).

We next questioned whether the monocyte expansion in *Lyn*<sup>-/-</sup> mice could be traced back to alterations in specific myeloid progenitor cell populations. BM from young (8–10 weeks) and aged (26–30 weeks) wt and *Lyn*<sup>-/-</sup> mice was harvested and numbers of myeloid progenitors, macrophage dendritic cell progenitor, and common monocyte progenitors (cMoP) were quantified. No significant differences between wt or *Lyn*<sup>-/-</sup> mice in either age group were observed (Figure 2A through 2C). We also found no significant difference in common dendritic cell progenitors (Figure 2C). Harder et al,<sup>47</sup> previously identified an increase in CSF-1 responsive progenitor cells in the spleens of *Lyn*<sup>-/-</sup> mice. Consistent with this, a significant increase (≈4-fold) in number of cMoPs was found

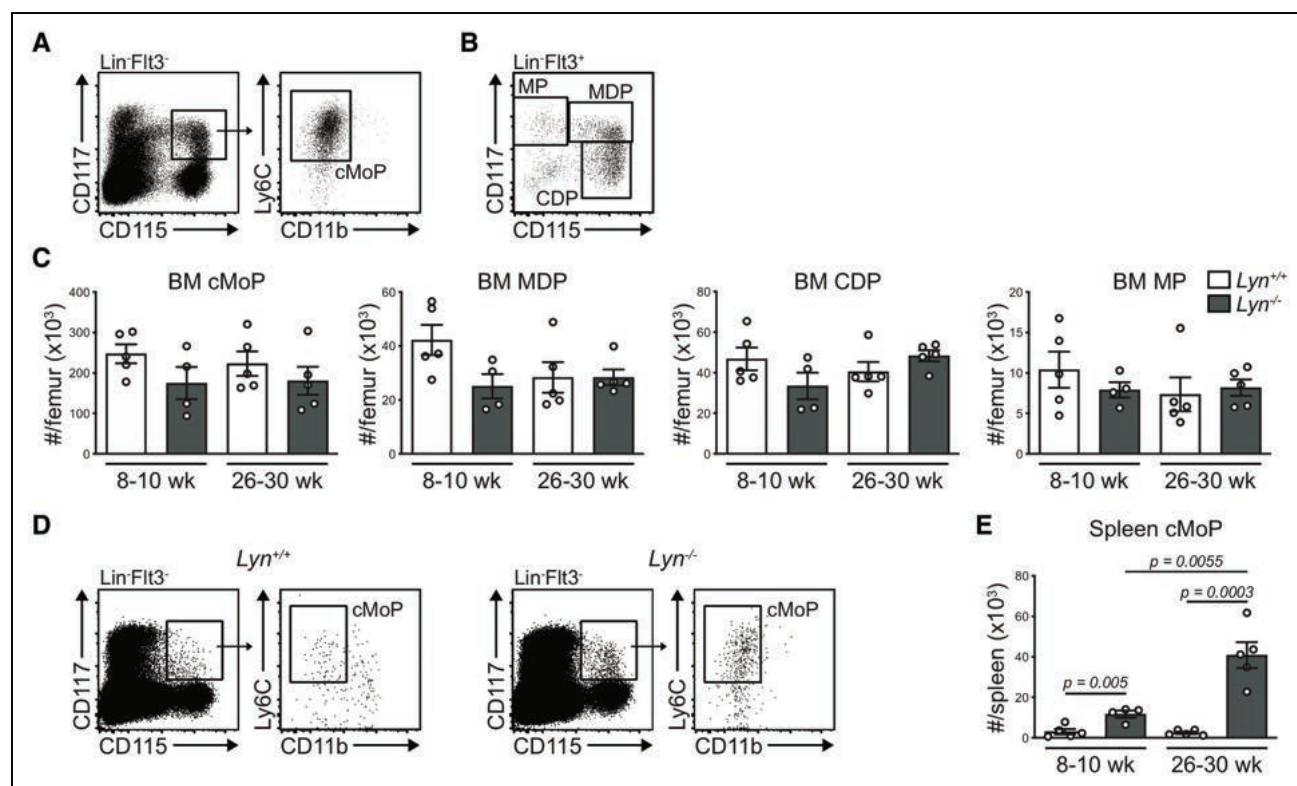


**Figure 2. *Lyn*<sup>-/-</sup> mice have increased numbers of splenic but not bone marrow (BM) monocyte progenitor cells.**

**A–C,** BM and **(D–E)** spleen were collected from young (8–10 wk) and aged (26–30 wk) naïve *Lyn*<sup>+/-</sup> and *Lyn*<sup>-/-</sup> mice, and progenitor cell populations were assessed by flow cytometry. **A, D,** and **E,** Common monocyte progenitors (cMoP) were identified as lineage<sup>-</sup> (CD3, CD19, NK1.1, Ly6G) Flt3<sup>+</sup>CD115<sup>+</sup>CD117<sup>+</sup>CD11b<sup>-</sup>Ly6C<sup>+</sup>. **B** and **C,** Macrophage dendritic cell progenitors (MDP), common DC progenitors (CDP), and myeloid progenitors (MP) were identified as lineage<sup>-</sup> (CD3, CD19, NK1.1, Ly6G, CD11b, CD11c, MHC II, Ter119, CD127) Flt3<sup>+</sup> and were distinguished as CD117<sup>+</sup>CD115<sup>+</sup>, CD117<sup>+</sup>CD115<sup>+</sup>, CD117<sup>+</sup>CD115<sup>-</sup>, respectively. **A, B,** and **D,** Representative plots are shown to demonstrate gating strategy. **C** and **E,** Graphs showing total number of indicated progenitor cells per femur or spleen. **A–C,** For MDPs, CDPs, and MPs data from a representative of at least 3 independent experiments are shown, n=4–5/group. For cMoPs, data from a representative of 2 independent experiments is shown, n=4–5/group. **D–E,** Data from an independent experiment is shown, n=4–5/group. Statistical significance was assessed using an unpaired Student *t* test. Data are mean±SEM.

in spleens of *Lyn*<sup>-/-</sup> mice that increased significantly with age (Figure 2D and 2E).

To investigate the consequence of increased LYN activity on the monocyte lineage we analyzed LYN gain-of-function (*Lyn*<sup>op</sup>) mutant mice.<sup>47</sup> Interestingly, increased LYN activity led to an overall increase in the frequency of monocytes in spleen and BM, as compared with wt mice. However, the frequency of cMos within total monocytes increased, while the frequency pMos decreased, in blood and BM of *Lyn*<sup>op</sup> mice (Figure IVA in the [Data Supplement](#)). There was also a decrease in the ratio of pMo/cMo in blood and BM (Figure IVB in the [Data Supplement](#)), resulting from a modest decrease in pMo numbers in blood and an increase in cMo in BM (Figure IVC and IVD in the [Data Supplement](#)). Therefore, although loss of LYN resulted in increased pMos, the reverse was not found in *Lyn*<sup>op</sup> mice, yet the overall ratio of pMo/cMo was decreased in *Lyn*<sup>op</sup> mice.

### Lyn Deficiency Impacts Monocyte Subset Composition, Surface Marker Expression, and Signaling

To better characterize monocyte populations and understand how LYN controls monocyte development, we assessed baseline signaling status of circulating monocyte populations within wt and *Lyn*<sup>-/-</sup> mice. To facilitate capture of steady-state signaling and monocyte subset identification, a panel of antibodies targeting cell surface proteins was selected based on capacity to retain binding/specificity following rapid fixation and RBC lysis. CyTOF was performed using these and phospho-specific antibodies targeting intracellular signaling proteins (Table II in the [Data Supplement](#)). To investigate whether LYN is a key regulator of pMos in general, or if its influence is restricted to a particular phenotypic subset, an Automatic Classification of Cellular Expression by Nonlinear Stochastic Embedding (ACCENSE) analysis<sup>53</sup> was performed on monocytes from wt and *Lyn*<sup>-/-</sup> mice. ACCENSE identified 20 distinct monocyte clusters, each with unique surface marker expression patterns, of which eleven had a pMo subset phenotype (clusters 2, 5, 6, 11, 12, 15, 16, 17, 18, 19, and 20), 6 a cMo phenotype (clusters 1, 7, 9, 10, 13, and 14), and 3 an intMo phenotype (clusters 3, 4, and 8; Figure 3A and 3B). Substantial differences in surface and phosphoprotein staining patterns were observed in wt cMos compared with pMos (eg, Ly6C, CD62L, pSTAT3 [cMos] and CD43, CD274, tyrosine phosphorylation [pTyr; pMos]). All cMos expressed Ly6C, whereas CD16/32, CD64 and CD62L were differentially expressed by cMo clusters. All pMo clusters expressed CD43 and FcγRIV to varying degrees, but differentially expressed CD274 (PD-L1), CD11c and Sca-1 (stem cell antigen 1, Ly6A). Hence, cMos and pMos have distinct surface marker expression

patterns with marked heterogeneity within the 2 main populations.

Analysis of signaling with phospho-specific antibodies identified significant differences in baseline signaling status of pMos compared with cMos clusters (Figure 3B). pMos exhibited higher levels of pTyr, pS6 and pSTAT1 (phospho-signal transducer and activator of transcription 1) but lower levels of pSTAT3, pp38, IκBα (NFκB inhibitor alpha), pERK1/2 (phospho-extra-cellular-related kinase 1/2), and pSTAT5 compared with cMos. Additionally, there were subtle differences in signaling patterns between various cMo and pMo clusters (Figure 3B). The MHC II<sup>+</sup> intMos (cluster 3) had a signaling signature resembling cMos rather than pMos. Indeed, ACCENSE analysis using just phosphoprotein markers to cluster monocytes clearly separated cMos and pMos subsets in t-distributed stochastic neighbor embedding space (Figure V in the [Data Supplement](#)).

Increased frequencies of various pMo clusters and a corresponding decrease in frequency of various cMo clusters (of total monocytes) was observed in *Lyn*<sup>-/-</sup> mice (Figure 3C and 3D). Loss of LYN did not lead to expansion of a particular subset of pMos but instead led to a general increase in various pMo clusters, with the most pronounced increase in CD274<sup>+</sup> pMos (clusters 16, 17, 18, and 20) compared with other pMo clusters (Figure 3C through 3G).

Loss of LYN was associated with increased CD115 (CSF-1R) expression and decreased CD43 expression on most monocyte clusters (Figure 3E). *Lyn* deficiency also dramatically impacted the signaling profile of monocytes, with the greatest difference observed in pMos. pTyr was significantly diminished in 8 of the 11 pMo clusters, and pSTAT1 levels were reduced in 6 of the pMo clusters. Wt pMos typically exhibited a higher pSTAT1 signal compared with wt cMos, but interestingly, this trend was reversed in the context of *Lyn* deficiency (Figure 3E). Together, these data identify LYN as an important negative regulator of a heterogeneous population of pMos and demonstrates that LYN governs select signaling pathways within these cells.

### Lyn Deficiency Causes Marked Perturbations Within the Transcriptomes of Monocytes

After investigating monocyte populations and signaling profiles in *Lyn*<sup>-/-</sup> mice, we were interested in understanding how LYN deficiency impacts monocyte gene expression. As we had observed marked heterogeneity within monocytes by CyTOF, we performed single cell RNA-sequencing on blood leukocytes from wt and *Lyn*<sup>-/-</sup> mice. Various myeloid and lymphoid immune cell subsets were identified in the blood of wt and *Lyn*<sup>-/-</sup> mice (Figure 4A and Table III.2 in the [Data Supplement](#)). Monocytes were identified based on their co-expression of *Csf1r* (CD115) and *Itgam* (CD11b), cMos selectively expressed *Ly6c2*



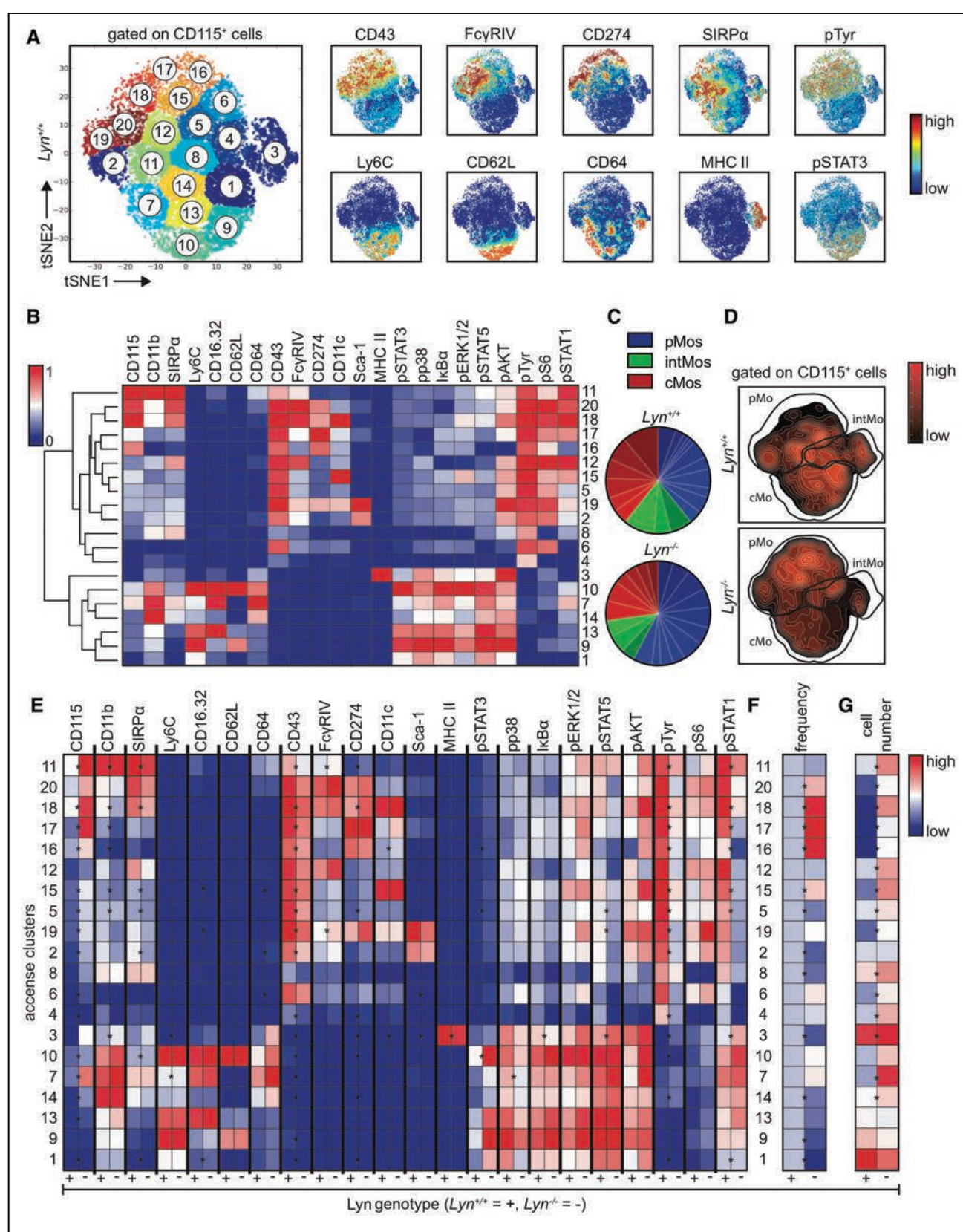


**Figure 3. LYN modulates monocyte composition, surface marker expression, and signaling.**

Blood from *Lyn*<sup>+/+</sup> (n=5) and *Lyn*<sup>-/-</sup> (n=5) mice was collected into RBC lysis/fixation buffer, and cells were analyzed by mass cytometry (CyTOF). **A**, Automatic Classification of Cellular Expression by Nonlinear Stochastic Embedding (ACCENSE) analysis was performed on *Lyn*<sup>+/+</sup> and *Lyn*<sup>-/-</sup> monocytes, with *Lyn*<sup>+/+</sup> monocyte heterogeneity depicted as 20 clusters (sig factor  $P=10^{-11}$ ). Smaller plots are colored according to signal intensity of the indicated markers. **B**, Relevant surface markers were used for clustering monocyte subsets using the Manhattan distance and average linkage method. (Continued)

(Ly6C) and pMos selectively expressed *Spn* (CD43) and *Fcgr4* (FcγRIV; Figure 4B). Consistent with our previous findings, there was an increase in circulating pMo abundance within *Lyn*<sup>-/-</sup> monocytes (Figure 4C).

We first sought to identify differentially expressed genes between wt cMos and wt pMos. More than 400 genes were differentially expressed between wt cMos and pMos (Figure 4D and Table III.3 in the [Data Supplement](#)). Consistent with previous work, we observed an upregulation of the transcription factors, *Nr4a1*, *Cebpb*, *Klf4*, and *Pou2f2* and the downregulation of *Fos* and *Irf7* in wt pMos compared with wt cMos.<sup>12,14</sup> Various negative regulators of apoptosis, such as the Bcl2 family members, were upregulated in pMos compared with cMos, consistent with their longer half-life.<sup>5</sup> pMos also upregulated the surface markers *Cd36*, *Cd9*, *Fcgr4*, and *Spn* and downregulated *Ccr2* and *Ly6c2* (Figure 4D and 4E).

After identifying the differentially expressed genes between the 2 major monocyte subsets in wt mice, we next analyzed transcriptomic changes in wt and *Lyn*<sup>-/-</sup> pMos (Table III.4 in the [Data Supplement](#)). Here, we observed that *Lyn*<sup>-/-</sup> pMos upregulated various genes encoding transcription factors compared with wt pMos, including *Fos*, *Jun*, *Junb*, *Nfat5*, and *Id2*, as well as *Nr4a1*, a critical transcription factor in pMos<sup>8,20</sup> (Figure 4F). Interestingly, no transcription factors were significantly downregulated in *Lyn*<sup>-/-</sup> pMos compared with wt. Additionally, a number of downstream targets of C/EBPβ, a key pMo transcription factor,<sup>11</sup> including *Clec4e*,<sup>54</sup> *S100a8*,<sup>55</sup> and *Pim1*<sup>56</sup> were upregulated in *Lyn*<sup>-/-</sup> pMos compared with wt. Heat shock family members, such as *Hspa1a*, *Hspa1b*, *Hsp90aa1*, and *Hsp90ab1*, were also upregulated in *Lyn*<sup>-/-</sup> pMos compared with wt pMos, as were other regulators of apoptosis such as *Pim1*, *Cdkn1a*, and *Cdkn1b*. *Lyn*<sup>-/-</sup> pMos also exhibited higher expression of genes associated with innate immunity including, *Cd9*, *Il1b*, and S100 family members *S100a8*, *S100a9*, and *S100a11* (Figure 4F and 4H).

As cMos are the obligate precursors of pMos,<sup>5,11,12</sup> we next looked at the genes differentially expressed in wt and *Lyn*<sup>-/-</sup> cMos (Table III.5 in the [Data Supplement](#)). *Nr4a1*, *Nr4a2*, *Fos*, *Jun*, and *Junb* were expressed at higher levels in *Lyn*<sup>-/-</sup> cMos. Similar to the differentially expressed genes between wt and *Lyn*<sup>-/-</sup> pMos, various negative regulators of apoptosis were also

differentially expressed between wt and *Lyn*<sup>-/-</sup> cMos. Lastly, as was seen in pMos, *Lyn*<sup>-/-</sup> cMos had a higher expression of C/EBPβ regulated genes including *Clec4e*, *S100a8*, and *Vcan*<sup>56</sup> compared with wt cMos (Figure 4G and 4I).

## LYN-Mediated Regulation of pMos Is Cell-Autonomous

We next questioned whether LYN was regulating monocytes in a cell-autonomous fashion, or whether altered LYN activity in other immune cells or nonhematopoietic cells impacted monocyte homeostasis. To assess LYN protein expression in vivo, blood and BM were harvested from naïve wt and *Lyn*<sup>-/-</sup> mice, and expression of LYN in monocytes and their precursors was assessed by flow cytometry, using *Lyn*<sup>-/-</sup> cells as a negative staining control. LYN was expressed in pMos and cMos in blood and BM (Figure 5A), and in myeloid progenitors, macrophage dendritic cell progenitors, and cMoPs, and by dendritic cell restricted progenitors, common dendritic cell progenitors (Figure 5B).

To determine whether LYN was playing a cell-intrinsic or extrinsic role in regulating monocyte development, we performed a series of experiments using BM-chimeras. First, CD45.1<sup>+</sup> mice, which express wt LYN, were lethally irradiated and transplanted with a mixture of BM cells that were 50% wt (CD45.1<sup>+</sup>) and 50% either wt, *Lyn*<sup>-/-</sup>, or *Lyn*<sup>flp</sup> (CD45.2<sup>+</sup>). This resulted in chimeric mice with wt *Lyn* in nonhematopoietic cells and a mixture of wt (CD45.1<sup>+</sup>) and wt or *Lyn* mutant (CD45.2<sup>+</sup>) leukocytes (Figure 5C in the [Data Supplement](#)). Mice transplanted with a mixture of wt CD45.2<sup>+</sup> and wt CD45.1<sup>+</sup> BM served as a control. In this setting, any differences observed in CD45.2<sup>+</sup> monocytes (wt, *Lyn*<sup>-/-</sup>, or *Lyn*<sup>flp</sup>), but not CD45.1<sup>+</sup> monocytes (wt) could be attributed to a cell-intrinsic role for LYN, whereas changes in CD45.1<sup>+</sup> monocytes would be a result of cell-extrinsic factors.

Analysis of monocyte populations in the mixed BM chimeric mice showed that monocytes derived from CD45.2<sup>+</sup> BM (wt, *Lyn*<sup>-/-</sup>, or *Lyn*<sup>flp</sup>) exhibited phenotypes consistent with monocytes in naïve wt, *Lyn*<sup>-/-</sup>, and *Lyn*<sup>flp</sup> mice, including an increased proportion of pMos within the *Lyn*<sup>-/-</sup> monocyte compartment in blood, BM, and spleen (Figure 5C). Importantly, mice transplanted with *Lyn*<sup>-/-</sup> CD45.2<sup>+</sup> BM had a significant increase in CD45.2<sup>+</sup>

**Figure 3 Continued.** The heatmap is colored based on signal intensity of the indicated markers. Min-max normalization was used on a per marker basis. **C**, Pie charts showing *Lyn*<sup>+/+</sup> and *Lyn*<sup>-/-</sup> monocyte ACCENSE cluster frequency. Clusters are grouped into patrolling monocytes (pMo; blue), intermediate monocytes (intMo; green), and cMos (red). **D**, Contour plots for the t-distributed stochastic neighbor embedding (t-SNE) coordinates of the *Lyn*<sup>+/+</sup> and *Lyn*<sup>-/-</sup> monocytes. The plots are colored using the monocyte cell density, and solid lines indicate the 3 major monocyte subsets. **E**, Heatmap showing relative signal intensities of the indicated cell surface and phosphoprotein/signaling markers among *Lyn*<sup>+/+</sup> and *Lyn*<sup>-/-</sup> monocyte ACCENSE clusters. Min-max normalization was used on a per marker basis. **F**, Heatmap showing the log2 transformed frequency and **G** the absolute numbers for each *Lyn*<sup>+/+</sup> and *Lyn*<sup>-/-</sup> monocyte ACCENSE cluster. For **E**, \* indicates statistical significance using SAM unpaired test ( $q < 0.01$ ). For **F** and **G**, \* indicates statistical significance using unpaired *t* test ( $P < 0.05$ ). FcγRIV indicates low-affinity immunoglobulin gamma Fc region receptor IV; IκBα, NFκB inhibitor alpha; MHC II, major histocompatibility complex class II; pERK1/2, phospho-extracellular-related kinase 1/2; pSTAT, phospho-signal transducer and activator of transcription; pTyr, phospho-tyrosine; and Sca-1, stem cell antigen 1.



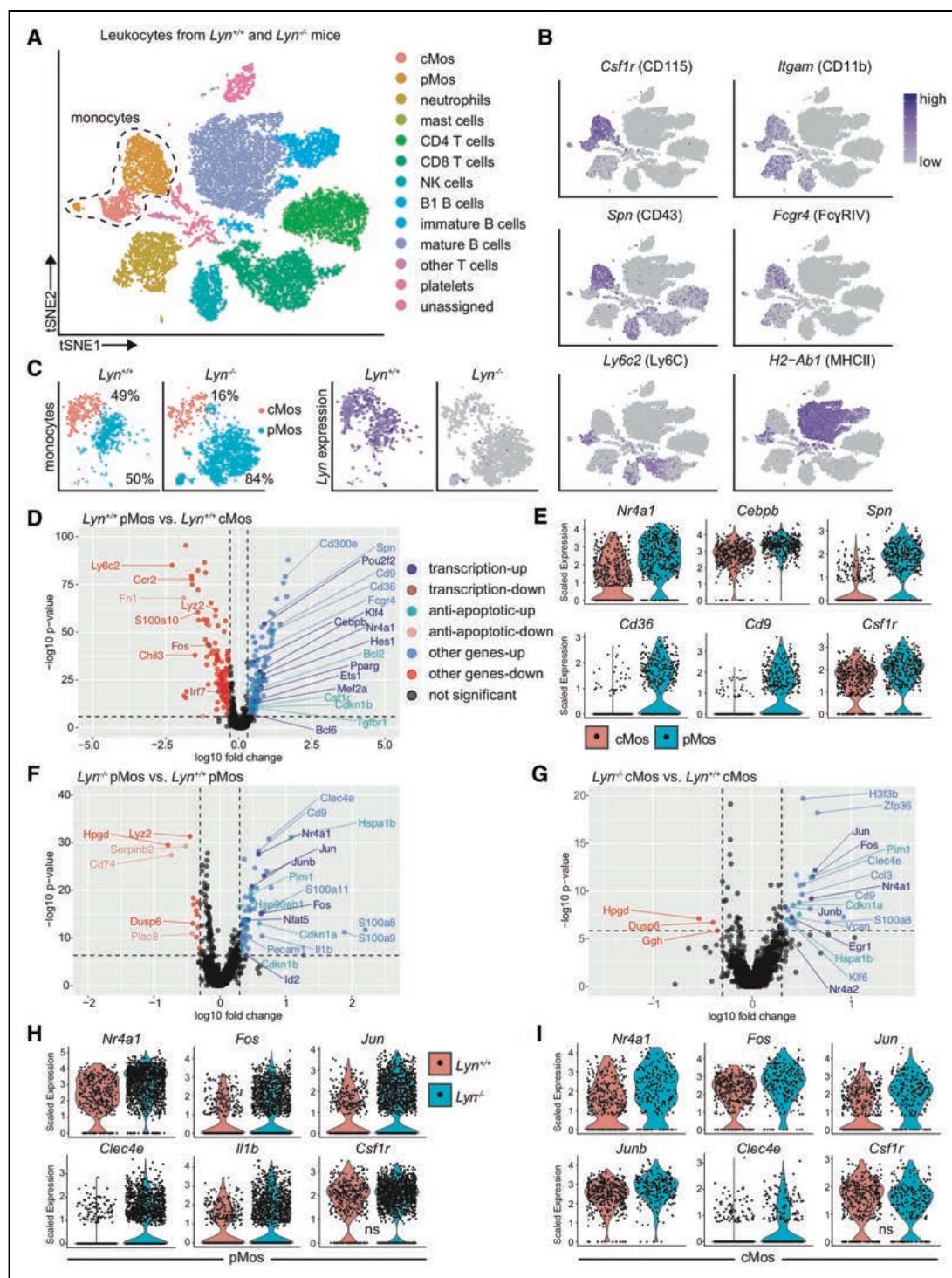


**Figure 4. LYN-deficiency impacts monocyte gene expression profiles.**

**A**, Single-cell transcriptomes of blood leukocytes were analyzed, and the indicated immune cell subsets were identified based on gene expression patterns. Black dotted line designates monocytes. **B**, viSNE plots are colored according to the expression of each gene. Grey and purple indicate maximum and minimum expression, respectively. **C**, Monocytes were reclustered based on gene expression and annotated as conventional monocytes (cMos) or patrolling monocytes (pMos). **Left**, The percent of each subset (cMo or pMo) within total monocytes is shown. **Right**, *Lyn* expression by wt and *Lyn*<sup>-/-</sup> monocytes is shown. Grey and purple indicate maximum and minimum expression, respectively. **D**, **F**, and **G**, Volcano plots depicting the average log fold change (avg\_logFC) vs the -log<sub>10</sub> P-value. The indicated genes were annotated based on their Biomart molecular function attribute for transcription factor activity (transcription) and the biological process attribute for negative regulator of apoptosis (anti-apoptotic). Blue and red indicate significantly upregulated and down regulated genes, respectively, identified using Wilcoxon ranked sum test and a threshold of absolute average log fold change (avg\_logFC) >0.3 and FDR corrected P value (*P*<sub>val\_adj</sub>) <0.05. Dashed black lines indicate the threshold cutoffs. **E**, **H**, and **I**, Violin plots of select genes are shown. All the genes are differentially expressed in **H** and **I** except for *Csf1r* as indicated by ns. Comparison of (**D** and **E**) wt (*Lyn*<sup>+/+</sup>) pMos and cMos, (**F** and **H**) wt and *Lyn*<sup>-/-</sup> pMos, and (**G** and **I**) wt and *Lyn*<sup>-/-</sup> cMos are shown. t-SNE, t-distributed stochastic neighbor embedding algorithm

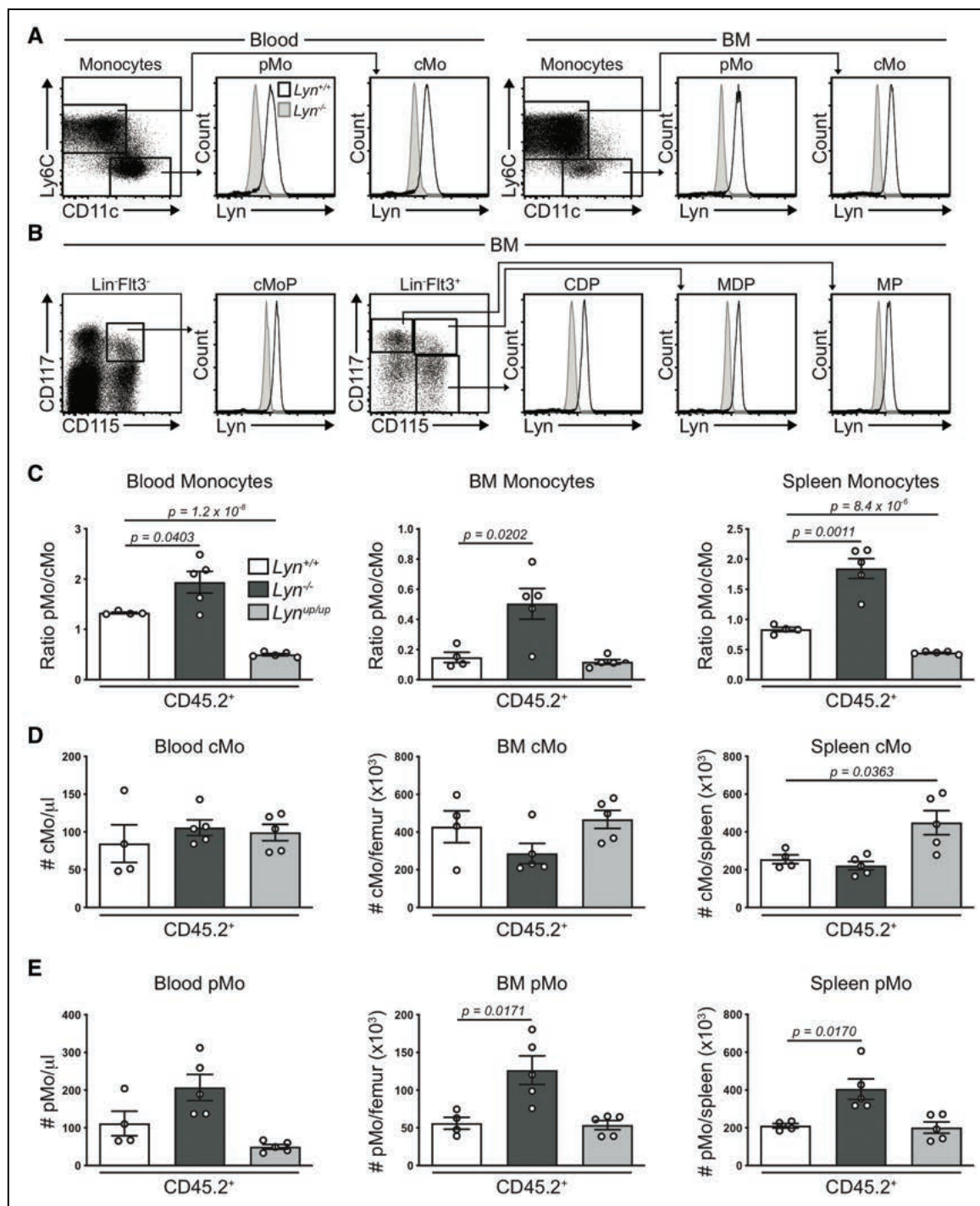


**Figure 5. LYN is expressed in all monocyte lineage cells and regulates patrolling monocyte populations in a cell-intrinsic manner.**

**A**, Blood and bone marrow (BM) were harvested from naïve *Lyn*<sup>+/+</sup> and *Lyn*<sup>-/-</sup> mice and LYN expression in **(A)** conventional monocytes (cMo; Ly6C<sup>+</sup>CD11c<sup>-</sup>) and patrolling monocytes (pMo; Ly6C<sup>-</sup>CD11c<sup>+</sup>), and **(B)** common monocyte progenitors (cMoP), macrophage dendritic cell progenitor (MDP), common DC progenitor (CDP), and myeloid progenitors (MP) was assessed by intracellular flow cytometry. **A** and **C-E**, Monocytes were identified as CD11b<sup>+</sup>CD115<sup>+</sup>Ly6G<sup>-</sup> and were gated based on FSC/SSC. **B**, cMoPs were identified as lineage<sup>-</sup> (CD3, CD19, NK1.1, Ly6G, CD11b<sup>-</sup>) Flt3<sup>-</sup>CD115<sup>+</sup>CD117<sup>+</sup>. MDPs, CDPs, and MPs were identified as lineage<sup>-</sup> (CD3, CD19, NK1.1, Ly6G, CD11b, CD11c, MHC II, Ter119, CD127) Flt3<sup>+</sup> and were distinguished as CD117<sup>+</sup>CD115<sup>+</sup>, CD117<sup>-</sup>CD115<sup>+</sup>, CD117<sup>+</sup>CD115<sup>-</sup>, respectively. **C-E**, Monocyte populations were assessed in radiation-chimeric mice 8 wk after reconstitution with a mixture of 50% *Lyn*<sup>+/+</sup> (CD45.1<sup>+</sup>) and 50% *Lyn*<sup>+/+</sup>, *Lyn*<sup>-/-</sup> or *Lyn*<sup>up/up</sup> (CD45.2<sup>+</sup>) BM. **C**, Ratios of pMo/cMo and total numbers of **(D)** cMo and **(E)** pMo per organ or  $\mu$ l of blood are shown. **A-B**, Representative data of 2 independent experiments are shown. **C-E**, Representative data of 2 independent experiments for *Lyn*<sup>+/+</sup> and *Lyn*<sup>-/-</sup> and an independent experiment for *Lyn*<sup>up/up</sup> mice are shown, n=4–5/group. Statistical significance was assessed using an unpaired Student *t* test. Data are mean $\pm$ SEM.

pMo numbers in BM and spleen and a trend towards increased CD45.2<sup>+</sup> pMos in blood, compared with mice transplanted with wt CD45.2<sup>+</sup> BM. Similar to the naïve *Lyn<sup>flp</sup>* mice, there was a trend towards decreased *Lyn<sup>flp</sup>* CD45.2<sup>+</sup> pMos in blood compared with CD45.2<sup>+</sup> wt controls (Figure 5E). No major differences in CD45.2<sup>+</sup> *Lyn<sup>-/-</sup>* cMo numbers were observed in mice transplanted with *Lyn<sup>-/-</sup>* BM; however, there were more splenic CD45.2<sup>+</sup> cMos in the *Lyn<sup>flp</sup>* group (Figure 5D).

To further investigate whether LYN's role in regulating monocyte subsets was cell-intrinsic, we examined the CD45.1<sup>+</sup> monocytes in the same chimeric mice. CD45.1<sup>+</sup> monocytes all express wt LYN, however, the groups differ in that they share their environment with wt, *Lyn<sup>-/-</sup>*, or *Lyn<sup>flp</sup>* immune cells. No difference in CD45.1<sup>+</sup> (wt) pMo numbers was observed in the presence or absence of *Lyn<sup>-/-</sup>* hematopoietic cells indicating that the pMo expansion observed in *Lyn<sup>-/-</sup>* CD45.2<sup>+</sup> cells was due to a cell-intrinsic role of LYN (Figure VIA in the [Data Supplement](#)). However, the presence of *Lyn<sup>-/-</sup>* hematopoietic cells resulted in a significant increase in proportion and number of wt (CD45.1<sup>+</sup>) cMos in blood and BM (Figure VIB and VIC in the [Data Supplement](#)). *Lyn<sup>flp</sup>* hematopoietic cells had no impact on the proportion or total numbers of wt (CD45.1<sup>+</sup>) cMos or pMos in any of the tissues analyzed (Figure VIA through VIC in the [Data Supplement](#)). Together, these data suggest that LYN acts as a cell-autonomous negative regulator of pMos.

To further assess whether LYN in nonhematopoietic cells could regulate monocytes in vivo, wt, *Lyn<sup>-/-</sup>*, and *Lyn<sup>flp</sup>* mice (CD45.2<sup>+</sup>), were lethally irradiated and transplanted with wt (CD45.1<sup>+</sup>) BM. Blood, BM, and splenic monocytes were then analyzed by flow cytometry, and no differences in monocyte composition were observed (Figure VIE through VIG in the [Data Supplement](#)). Overall, we conclude that although LYN is expressed in various cell types that could influence monocyte homeostasis, LYN primarily regulates monocyte populations through cell-intrinsic mechanisms.

## LYN Is a Negative Regulator of CSF-1-Induced Monocyte Development and Survival In Vitro

Given the cell-autonomous role for LYN in regulating pMos in vivo, the elevated expression of CSF-1R (CD115) on circulating *Lyn<sup>-/-</sup>* pMos (Figure 3E), the dependence of pMo homeostasis on CSF-1,<sup>5</sup> and previous studies defining LYN as a negative regulator of CSF-1R signaling in BM-derived macrophages,<sup>57,58</sup> we hypothesized that LYN may negatively regulate pMo populations by inhibiting responses to CSF-1. To begin to address this, we developed an in vitro culture system to generate BM-derived monocytes (BM-Mo). BM was grown in culture for 7 to 9 days under nonadherent conditions with media supplemented with CSF-1. Analysis by flow cytometry indicated that the cells were phenotypically similar to pMos in vivo. More than 90% of the cells co-expressed CD11b and

CD115 (CSF-1R), and, of those, 95% expressed CD11c and CD274, and lacked expression of Ly6C and CD62L (Figure 6A). Consistent with previous studies of LYN in BM-macrophages,<sup>46,47</sup> *Lyn<sup>-/-</sup>* BM cultures produced increased BM-Mo numbers compared with wt (Figure 6B). Since LYN and SFKs have been identified as negative regulators of CSF-1R induced survival pathways,<sup>57,58</sup> we questioned whether *Lyn<sup>-/-</sup>* BM-Mos had increased survival in limiting concentrations of CSF-1. Wt and *Lyn<sup>-/-</sup>* BM-Mos were collected after 7 days of culture, and equal numbers of cells were plated in varying concentrations of CSF-1. Cell survival was then assessed by counting viable cells after 2 and 5 days of culture. Significantly more *Lyn<sup>-/-</sup>* BM-Mos were recovered at both times, when cultured with 10 and 2 ng/mL of CSF-1 (Figure 6C). Together, these data support the role for LYN as a negative regulator of CSF-1-dependent monocyte development and survival.

## LYN Regulates pMo Population Dynamics and Expression of CSF-1R In Vivo

CSF-1 plays an important role in mediating monocyte homeostasis and is thought to regulate the circulating half-life of pMos in vivo.<sup>5</sup> CyTOF analysis of CSF-1R (CD115) expression on circulating wt and *Lyn<sup>-/-</sup>* monocytes (Figure 3E) revealed higher CSF-1R expression on *Lyn<sup>-/-</sup>* monocytes. Analysis of blood, BM, and splenic monocyte CSF-1R (CD115) levels by flow cytometry confirmed that *Lyn<sup>-/-</sup>* pMos and cMos expressed significantly higher levels of CSF-1R in all of these tissues (Figure 6D). Given the increased numbers of pMos observed in *Lyn<sup>-/-</sup>* mice and the established role of CSF-1 in regulating monocyte survival in vivo, we questioned whether LYN regulates monocyte circulating half-life. Wt and *Lyn<sup>-/-</sup>* mice were treated with fluorescent (Dil) lipid nanoparticles, which uniformly label phagocytic cells including monocytes, and the presence of Dil<sup>+</sup> circulating monocytes was assessed over time by flow cytometry. Almost 100% of monocytes were Dil<sup>+</sup> up to 3 days following Dil-lipid nanoparticle injection (Figure 6E and 6F). After 5 days, ~45% of wt cMos were Dil<sup>+</sup>, while Dil<sup>+</sup> cMos were absent by day 8, consistent with the short circulating half-life of cMos.<sup>5</sup> *Lyn<sup>-/-</sup>* cMos had a slight increase in turnover with only ~20% Dil<sup>+</sup> cMos by day 5 (Figure 6E). By contrast, *Lyn<sup>-/-</sup>* pMos had a significantly longer circulating half-life (5.3 days) than wt pMos (2.7 days) with almost 30% of *Lyn<sup>-/-</sup>* pMos remaining Dil<sup>+</sup> 18 days after labeling (Figure 6F).

To extend this analysis, we used a bromodeoxyuridine (BrdU) labeling approach, where BrdU is incorporated into the DNA of dividing progenitor cells, and is inherited by newly developed cMos, which then differentiate into BrdU<sup>+</sup> pMos. Consistent with results by Yona et al,<sup>5</sup> the majority of cMos were BrdU<sup>+</sup> 2 days post treatment, with BrdU lost by day 6 (Figure 6G). By contrast, pMos remained mostly BrdU<sup>-</sup>, with a peak of ~12% BrdU<sup>+</sup> at day 4 post-injection in wt pMos,



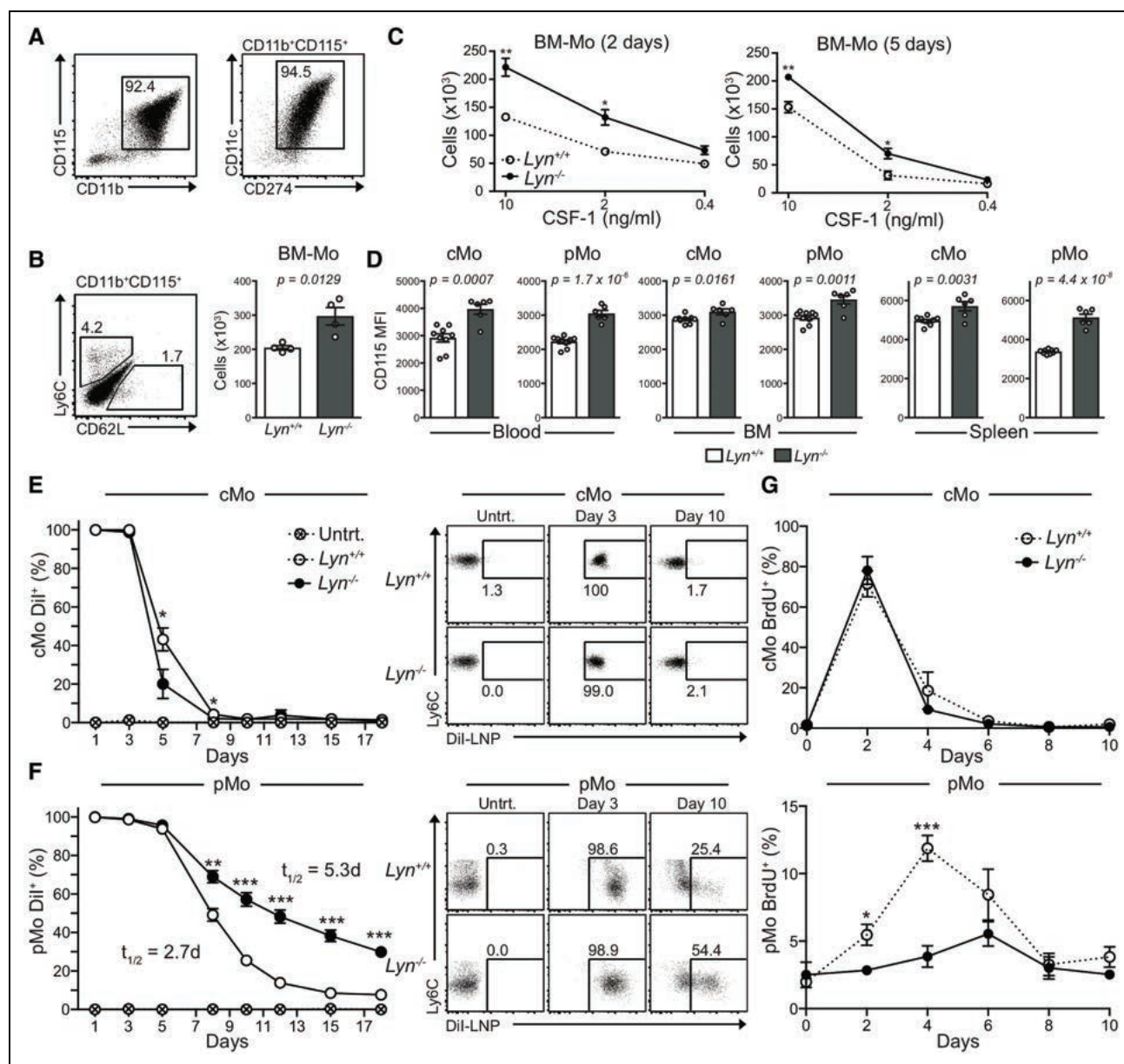


**Figure 6. LYN negatively regulates monocyte development in response to CSF-1 (colony stimulating factor-1) in vitro and regulates circulating patrolling monocyte (pMo) half-life.**

**A–C.** Bone marrow-derived monocytes (BM-Mo) were grown in vitro. **A**, Cell subsets were analyzed by flow cytometry on day 7. Representative plots are shown, and numbers indicate frequency of gated populations. **B**, Total number of cells per well on day 7 are shown. **C**, After 7 days in culture, equal numbers of cells were replated with the indicated concentrations of CSF-1. The number of live cells per well was assessed 2 and 5 days later. **D**, Blood, BM, and spleen were collected from naïve *Lyn*<sup>+/+</sup> and *Lyn*<sup>-/-</sup> mice and CD115 surface expression on conventional monocytes (cMos; Ly6C<sup>+</sup>CD62L<sup>+</sup>) and pMos (Ly6C<sup>-</sup>CD62L<sup>-</sup>) was assessed by flow cytometry. Graphs represent geometric mean fluorescent intensity (MFI) for the indicated Mo subsets. **E–G**, *Lyn*<sup>+/+</sup> and *Lyn*<sup>-/-</sup> mice were treated with (**E–F**) Dil-lipid nanoparticle (LNP) or (**G**) BrdU. Presence of Dil<sup>+</sup> or BrdU<sup>+</sup> blood monocyte populations were assessed by flow cytometry at the indicated time points. Representative plots are shown for cMo (CD115<sup>+</sup>Ly6C<sup>+</sup>CD11c<sup>+</sup>) and pMo (CD115<sup>+</sup>Ly6C<sup>-</sup>CD11c<sup>+</sup>) and numbers indicate frequency of Dil<sup>+</sup> cells. Graphs represent frequency of Dil<sup>+</sup> or BrdU<sup>+</sup> cMo and pMo over time. **A–C**, Representative data from at least 3 independent experiments are shown, (**B**)  $n=4$ /group, (**C**)  $n=3$ /group. **D**, Representative data from 3 independent experiments are shown,  $n=6$ /group. **E–G**, Representative data from 2 independent experiments for each treatment type are shown,  $n=5$ –6/group. Statistical significance was assessed using an unpaired Student *t* test. Data are mean $\pm$ SEM.

consistent with their significantly longer circulating half-life compared with cMos.<sup>5,59</sup> No differences in BrdU incorporation kinetics were observed in cMo populations between wt and *Lyn*<sup>-/-</sup> mice. Interestingly, *Lyn*<sup>-/-</sup> pMos exhibited a significant reduction in BrdU

incorporation compared with wt, suggesting a slower rate of turnover of these cells (Figure 6G). Together, these data identify LYN as a negative regulator of circulating pMo half-life and monocyte CSF-1R expression in vivo.

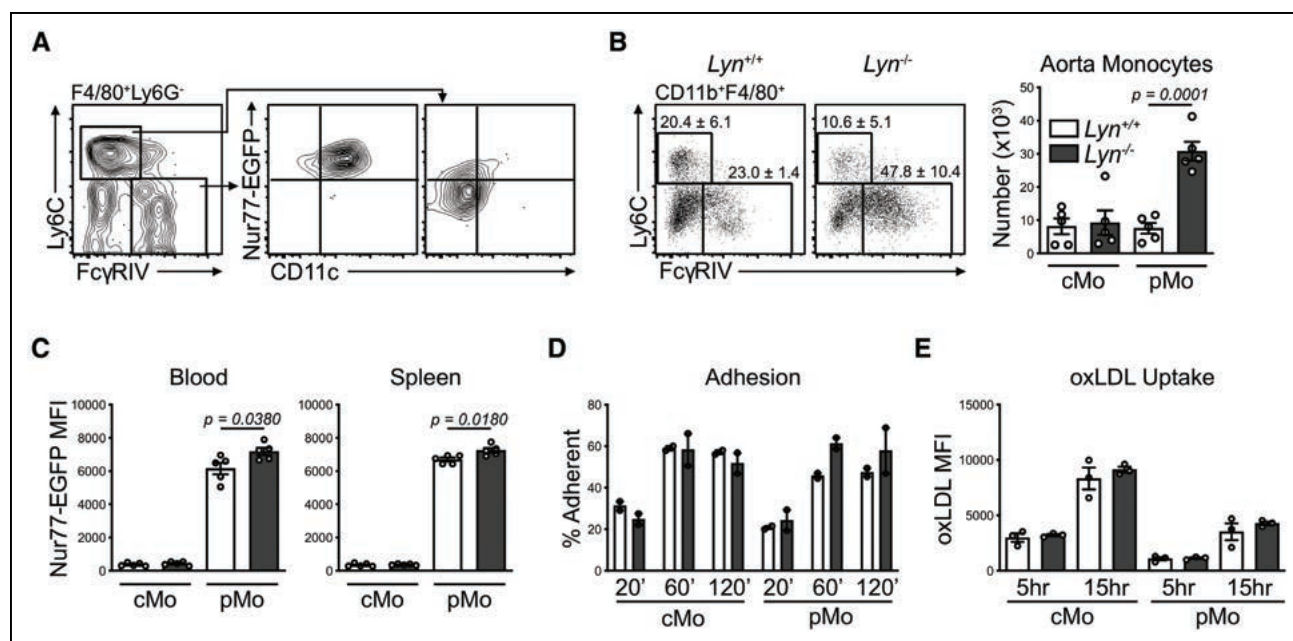


**Figure 7. *Lyn* deficiency leads to an increase in aortic patrolling monocytes (pMos) and does not impair pMo function.**

**A–B,** Aortas were harvested from naïve **(A)** Nur77<sup>EGFP</sup> ( $n=6$ ), **(B)** *Lyn*<sup>+/+</sup> and *Lyn*<sup>-/-</sup> mice ( $n=5$ ) and conventional monocytes (cMos) and pMos were assessed by flow cytometry according to the indicated gating strategy. Cells were first gated on live CD45<sup>+</sup> cells. **C,** Blood and spleen were harvested from Nur77<sup>EGFP</sup> wt and Nur77<sup>EGFP</sup> *Lyn*<sup>-/-</sup> mice and expression of Nur77 (EGFP) was assessed in cMos and pMos by flow cytometry ( $n=5$ ). **D,** White blood cells from *Lyn*<sup>+/+</sup> ( $n=3$ ) and *Lyn*<sup>-/-</sup> ( $n=3$ ) were incubated on a confluent layer of murine endothelial cells for the indicated times. Percent adhesion indicates the proportion of monocytes in the adherent fraction relative to total. **E,** White blood cells from naïve *Lyn*<sup>+/+</sup> or *Lyn*<sup>-/-</sup> mice were incubated with fluorescent oxLDL (oxidized low-density lipoprotein). Uptake of oxLDL by cMos and pMos was assessed at the indicated times by flow cytometry ( $n=3$ ). Representative data from **(D)** 3 or **(A, C, and E)** 2 independent experiments is shown. Statistical significance was assessed using an unpaired Student *t* test. Data are mean ± SEM.

## Lyn Deficiency Is Protective in the *Ldlr*<sup>-/-</sup> High-Fat Diet Model of Atherosclerosis

Monocytes play a central role in the development and progression of atherosclerosis,<sup>37–39</sup> and recent studies have shown that mice lacking pMos develop more severe atherosclerosis.<sup>23,24,60</sup> Given the significantly increased numbers of pMos in *Lyn*-deficient mice, we questioned whether *Lyn*<sup>-/-</sup> mice might be protected from atherosclerosis. We first addressed whether *Lyn*<sup>-/-</sup> mice had an altered aortic monocyte compartment. Aortas were harvested from naïve wt and *Lyn*<sup>-/-</sup> mice and F4/80<sup>+</sup> cells (includes monocytes and macrophages) were assessed by flow cytometry. Aortic cMos/cMo-derived cells (herein referred to as cMos) were defined as Ly6C<sup>+</sup>FcγRIV<sup>-</sup>, and pMos/pMo-derived cells (pMos) were Ly6C<sup>+</sup>FcγRIV<sup>+</sup>. Consistent with these phenotypes, pMos but not cMos, exhibited high Nur77 expression (using reporter mice expressing enhanced green fluorescent protein [EGFP] under the Nur77 promoter [Nur77<sup>EGFP</sup>]) and were CD11c<sup>+</sup> (Figure 7A). *Lyn*<sup>-/-</sup> mice had significantly more (~4-fold) aortic pMos than wt mice, with no difference in cMo populations (Figure 7B). Consistent with the single cell RNA-sequencing data (Figure 4F and 4H), *Lyn*<sup>-/-</sup> pMos in blood and spleen had a significant increase in Nur77-EGFP reporter expression compared with their wt counterparts; however, no difference in Nur77-EGFP

expression was observed between wt and *Lyn*<sup>-/-</sup> cMos (Figure 7C).

We reasoned that functional differences in *Lyn*<sup>-/-</sup> monocytes might affect their numbers in circulation and propensity to adhere to the vasculature and contribute to the development and progression of atherosclerosis. To test monocyte adhesion, wt and *Lyn*<sup>-/-</sup> blood leukocytes were incubated on b.END3 endothelial cell monolayers, and the proportion of adherent and nonadherent cells were assessed by flow cytometry. Loss of LYN had no impact on adhesion of cMos or pMos, as similar proportions of wt and *Lyn*<sup>-/-</sup> monocytes adhered to endothelial cells (Figure 7D). Thus, we did not detect a difference in the intrinsic adhesion of *Lyn*<sup>-/-</sup> pMos that might explain their greater circulatory or aorta-associated numbers.

We next tested the uptake of oxLDL (oxidized low-density lipoprotein) by monocytes as this is a key driver in the development of atherosclerosis. Wt and *Lyn*<sup>-/-</sup> monocytes were incubated with fluorescently labelled oxLDL, and its binding/uptake was assessed by flow cytometry. We found that cMos had an increased capacity to take-up oxLDL as compared with pMos, but the loss of LYN did not affect the levels of oxLDL in either subset (Figure 7E).

Finally, to determine the impact that increased numbers of pMos might have on susceptibility to atherosclerosis, we used the *Ldlr*<sup>-/-</sup> high-fat diet model of

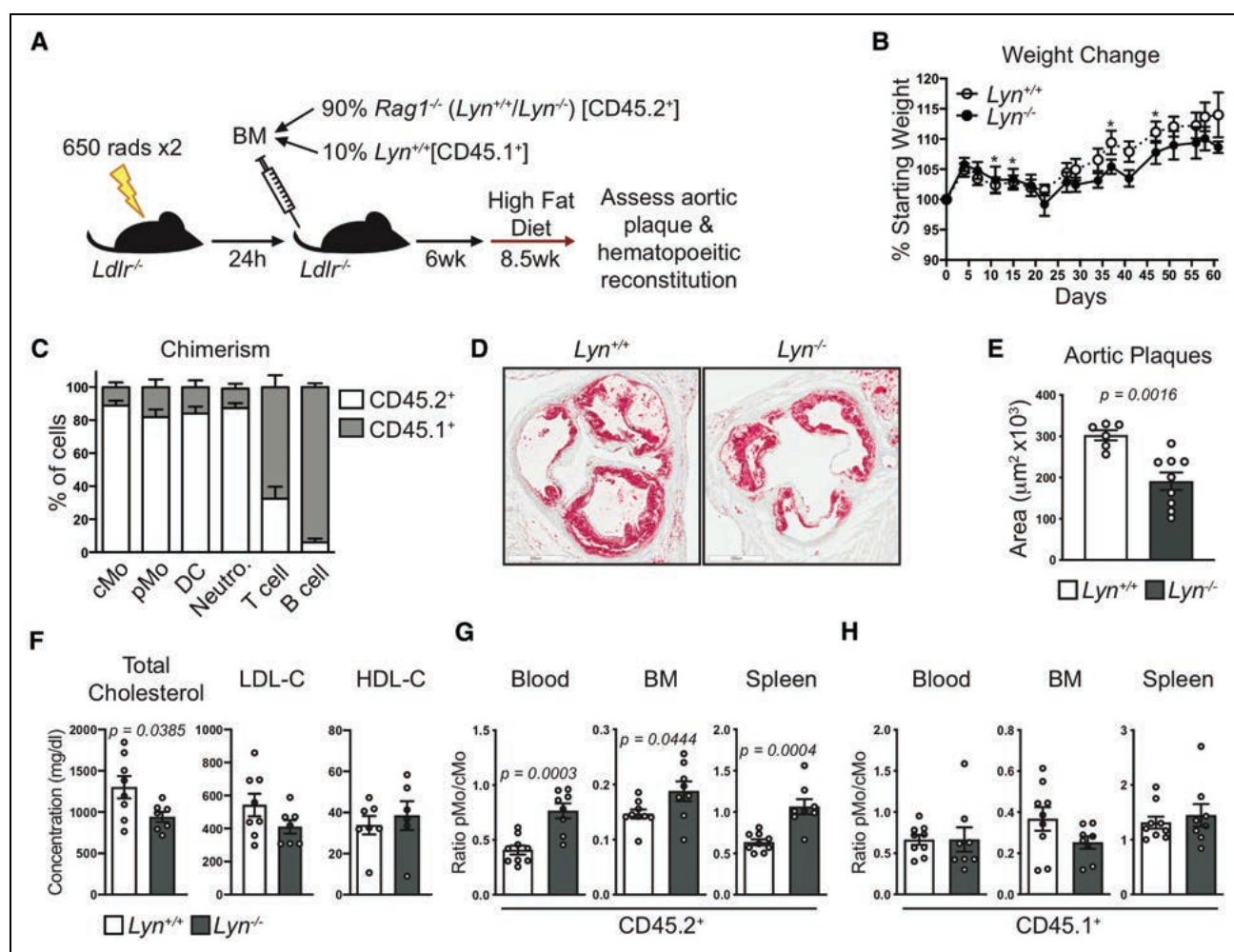


**Figure 8. *Lyn* deficiency diminishes high-fat diet-induced atherosclerosis in *Ldlr*<sup>-/-</sup> mice.**

Lethally irradiated *Ldlr*<sup>-/-</sup> mice were transplanted with 10% *Lyn*<sup>+/+</sup> (CD45.1<sup>+</sup>) bone marrow (BM) as a source of wt adaptive immune cells together with 90% *Rag1*<sup>-/-</sup> or *Rag1*<sup>-/-</sup>*Lyn*<sup>-/-</sup> (CD45.2<sup>+</sup>) BM to reconstitute the innate immune compartment with either *Lyn*<sup>+/+</sup> or *Lyn*<sup>-/-</sup> BM-derived cells. Six weeks later mice were given a high-fat diet to induce atherosclerosis and 8.5 wk later blood, BM, spleen, and heart/aortic root were harvested. **A**, A schematic representation of the experimental protocol. **B**, Chimerism was confirmed in blood cells by flow cytometry. Graph represents frequency of CD45.1<sup>+</sup> and CD45.2<sup>+</sup> cells within conventional monocytes (cMo; CD11b<sup>+</sup>CD115<sup>+</sup>Ly6C<sup>+</sup>CD62L<sup>+</sup>), patrolling monocyte (pMo; CD11b<sup>+</sup>CD115<sup>+</sup>Ly6C<sup>+</sup>CD62L<sup>-</sup>), dendritic cells (DC; CD11c<sup>+</sup>MHC II<sup>+</sup>), neutrophils (CD11b<sup>+</sup>Gr1<sup>hi</sup>), T cells (CD3<sup>+</sup>CD19<sup>-</sup>), and B cells (CD19<sup>+</sup>CD3<sup>-</sup>). **C**, Mice were weighed twice weekly during high-fat diet treatment. **D**, Aortic roots were cross-sectioned and stained with Oil Red O to visualize atherosclerotic plaques, and **(E)** Plaque area was quantified. **F**, Serum lipid levels (total cholesterol, LDL-C [low-density lipoprotein cholesterol] and HDL-C [high-density lipoprotein cholesterol]) were measured at the experimental end point. **G**, CD45.2<sup>+</sup> and **H**, CD45.1<sup>+</sup> cMo and pMo in blood, BM, and spleen were assessed by flow cytometry. Graphs represent ratio of pMo/cMo. For **F**, data from an independent experiment is shown, and for the rest, representative data from 2 independent experiments is shown, n=6–9/group. Statistical significance was assessed using an unpaired Student *t* test. Data are mean±SEM. MHC II indicates major histocompatibility complex class II.

atherosclerosis.<sup>37,61</sup> *Lyn* deficiency in the innate immune system was achieved by generating mixed BM chimeric mice in *Ldlr*<sup>-/-</sup> hosts, in an effort to eliminate the potential impact of *Lyn*-deficient adaptive immune cells (eg, B cells). *Ldlr*<sup>-/-</sup> (CD45.2<sup>+</sup>) recipients were injected with a mixture of 10% wt (CD45.1<sup>+</sup>) BM together with 90% either *Rag1*<sup>-/-</sup> or *Rag1*<sup>-/-</sup>*Lyn*<sup>-/-</sup> BM (CD45.2<sup>+</sup>, cannot produce B or T cells), and atherosclerosis was induced in chimeric mice by providing a high-fat diet for 8.5 weeks (Figure 8A). The resulting chimeric mice lacked low-density lipoprotein receptor expression in nonhematopoietic cells and possessed wt CD45.1<sup>+</sup> adaptive immune cells.

By contrast, the majority (~90%) of innate immune cells, including monocytes, were derived from *Rag1*<sup>-/-</sup> BM and were, therefore, either wt or *Lyn*-deficient and could be distinguished from wt-derived immune cells by the congenic marker CD45.2. Chimerism was assessed by flow cytometry and innate immune cells were ~90% CD45.2<sup>+</sup> (Figure 8B). Furthermore, B cells were ~95% CD45.1<sup>+</sup>, indicating successful chimerism, and T cells were ~70% CD45.1<sup>+</sup>, consistent with the radio-resistant nature of some T cells and their progenitors.<sup>62–64</sup>

Mice were weighed twice weekly on the high-fat diet, and, after an initial drop in weight, all mice steadily gained



weight (Figure 8C). Atherosclerotic plaque area in the aortic root was quantified using Oil Red O staining. Mice reconstituted with *Lyn*<sup>-/-</sup> BM had significantly reduced plaque area compared with their wt counterparts, indicating that loss of LYN in innate immune cells protects *Ldlr*<sup>-/-</sup> mice from high-fat diet-induced atherosclerosis (Figure 8D and 8E). Serum from *Lyn*<sup>-/-</sup> chimeric mice had significantly lower levels of total cholesterol at the experimental end point, with a trend of decreased LDL cholesterol, and no differences in HDL-cholesterol (Figure 8F). Protection from atherosclerosis in *Lyn*<sup>-/-</sup> chimeric mice correlated with increased proportions of *Lyn*<sup>-/-</sup> pMos within the monocyte compartment in blood, BM, and spleen (Figure 8G). Furthermore, consistent with mixed BM chimeras in a nonatherogenic setting (Figure 5 and Figure VI in the [Data Supplement](#)), these changes were cell-intrinsic as wt (CD45.1<sup>+</sup>) monocytes in the same recipient mice did not exhibit differences in monocyte subset composition (Figure 8H). Overall, these data demonstrate that loss of LYN in innate immune cells acts to antagonize atherosclerosis, a phenotype associated with increased systemic and aorta-associated pMos.

## DISCUSSION

The LYN tyrosine kinase is a well-established negative regulator of myeloid cell development and function<sup>46–49,65,66</sup>; however, the role of LYN in Mo subset development has not been investigated. The study presented here identifies a novel role for LYN as a negative regulator of pMo homeostasis and provides important clarification regarding LYN's role in monocytes. Previous studies that identified increased monocyte numbers in *Lyn*<sup>-/-</sup> mice were performed before the discovery of pMos as a unique monocyte subset.<sup>46,47</sup> Therefore, the increase in monocytes in *Lyn*<sup>-/-</sup> mice was assumed to be an increase in cMo numbers. However, here we show that, except for increased splenic cMos in aged *Lyn*<sup>-/-</sup> mice, *Lyn* deficiency in monocytes does not lead to increased cMos, but instead results in a significant increase in pMos in blood, BM, spleen, and aorta. This increase in pMos in *Lyn*<sup>-/-</sup> mice is independent of myeloproliferative disease and the adaptive immune system, suggesting a steady-state role for LYN in regulating pMo population size. We did not observe differences in BM progenitor numbers, but spleens from young and aged *Lyn*<sup>-/-</sup> mice had a significant expansion of cMoPs, indicating extramedullary monopoiesis might contribute to systemic pMo expansion in these mice. This is consistent with previous studies showing increased splenic progenitors with myeloid differentiation capacity in *Lyn*<sup>-/-</sup> mice.<sup>46,47,65</sup> Although cMos have been identified as obligate precursors to pMos in blood, whether pMos can develop directly from BM or splenic precursors remains unclear.<sup>25</sup> An investigation of the role of splenic cMoPs in the development

of pMos might provide valuable insight into pMo biology and, given the increase in extramedullary myelopoiesis and cMoPs in *Lyn*<sup>-/-</sup> mice, these mice could be a useful model to study this process.

LYN may also regulate pMo populations by limiting their survival as *Lyn*<sup>-/-</sup> pMos were found to have almost double the circulating half-life as their wt counterparts. This was supported by upregulation of number of genes encoding negative regulators of apoptosis in *Lyn*<sup>-/-</sup> pMos compared with their wt counterparts. The molecular mechanisms regulating pMo development and survival are still largely unclear, however, Nur77, C/EBPβ, and CSF1-R signaling have all been identified as important regulators of pMo differentiation and survival.<sup>8,11,34</sup> The data presented here suggest that LYN may play an important regulatory role in these pathways, including as a negative regulator of *Nr4a1* (encodes Nur77) expression. C/EBPβ was recently shown to be a key regulator of pMo biology, by regulating their survival and by promoting their differentiation from cMo precursors.<sup>11,33</sup> The transcriptional data presented here revealed a possible role for LYN in regulating C/EBPβ activity throughout the monocyte lineage as a number of C/EBPβ regulated genes, including *Nr4a1*<sup>11</sup>, were upregulated in *Lyn*<sup>-/-</sup> cMos and pMos compared with their wt counterparts. Interestingly, C/EBPβ regulates expression of both *Nr4a1* and *Csf1r* in monocytes further highlighting its importance as a key regulator of monocyte biology.<sup>11,33</sup> LYN's role in regulating C/EBPβ activity in monocytes, therefore, warrants further investigation.

Although we did not observe differences in *Csf1r* expression in *Lyn*<sup>-/-</sup> monocytes, CSF-1R (CD115) was significantly upregulated on the surface of *Lyn*-deficient cMos and pMos. Surface CSF-1R expression is regulated by a variety of post-transcriptional mechanisms including ligand binding-induced receptor internalization, and our data suggest LYN plays a role in one or more of these mechanisms. In line with this, LYN and SFKs have been implicated in CSF-1R signaling in at least 2 recent studies. Baran et al,<sup>57</sup> found that LYN negatively regulates CSF-1R signaling in BM-macrophages by promoting activity of the inhibitory phosphatase SHIP-1 (Src homology 2 domain containing inositol polyphosphate 5-phosphatase 1). Another study found that SFK binding to the juxtamembrane domain of CSF-1R resulted in receptor internalization and degradation in response to ligand binding.<sup>58</sup> Consistent with a role for LYN as a negative regulator of monocyte survival downstream of CSF-1R signaling, we found that *Lyn*<sup>-/-</sup> BM-derived monocytes had increased survival in limiting CSF-1 concentrations in vitro. Furthermore, the increased CSF-1R (CD115) surface expression on *Lyn*<sup>-/-</sup> monocytes is consistent with SFK driven receptor internalization and degradation and could result in prolonged or increased CSF-1R signaling in *Lyn*<sup>-/-</sup> monocytes. Interestingly, although *Lyn*<sup>-/-</sup> cMos also exhibited higher CSF-1R expression, no major differences in *Lyn*<sup>-/-</sup> cMo population turnover was observed.

Therefore, while LYN-mediated regulation of CSF-1R signaling may alter pMo populations, it does not seem to have a profound effect on cMos. This is consistent with increased reliance on CSF-1R signaling in pMos versus cMos.<sup>67</sup> Although, cMos require CSF-1R signaling for their development, as evidenced by substantial loss of monocytes in CSF-1 and CSF-1R deficient mice,<sup>68,69</sup> prolonged neutralization of the receptor does not result in a loss of cMos, while it dramatically affects pMos.<sup>67</sup> Therefore, if LYN acts to inhibit CSF-1R signaling, it is not surprising that the phenotype manifests more dramatically in pMo numbers.

Here, we used CyTOF coupled with ACCENSE to characterize circulatory monocyte phenotype, subset heterogeneity, and signaling properties. This deep phenotyping approach allowed us to decipher the heterogeneity in surface marker expression profiles and signaling patterns in monocytes at steady state and in the context of *Lyn* deficiency. Importantly, this approach revealed very distinct phosphoprotein signaling signatures distinguishing cMos from pMos. For example, pMos were pTyr<sup>hi</sup> pSTAT3<sup>low</sup> while cMos displayed the reverse characteristics. We found that LYN acts as a negative regulator of pMo numbers across the range of phenotypic clusters, with loss of LYN resulting in a failure to acquire wt levels of pTyr and pSTAT1 in pMos. These results clearly show that LYN is a key tyrosine kinase controlling pMo signaling patterns. Consistent with a role for LYN as a key regulator of numerous signal transduction pathways regulating monocyte biology, numerous transcription factors were differentially expressed in the absence of LYN. Mass spectrometry based phospho-proteomic analyses of wt and *Lyn*<sup>-/-</sup> pMos will be crucial for identifying targets of LYN kinase activity in pMos and determining how changes in these signaling pathways regulate pMo gene expression patterns as well as their number and lifespan.

Conventional monocytes are well-established drivers of atherosclerosis in humans whereas numerous experimental models of disease have shown that loss of pMos exacerbates atherosclerosis.<sup>23,60,70</sup> However, relatively little is known about how SFKs regulate these processes. Although numerous members of the SFK family are expressed throughout the innate immune system, Fgr, Hck, and Lyn are thought to be the 3 major SFKs active in monocytes and macrophages.<sup>71</sup> A recent study by Medina et al<sup>72</sup> investigated the role of HCK (hemopoietic cell kinase) and FGR (feline Gardner-Rasheed sarcoma viral oncogene homolog) in monocytes and atherosclerosis. In this study, deficiency of both HCK (hemopoietic cell kinase) and FGR (feline Gardner-Rasheed sarcoma viral oncogene homolog) in immune cells led to a decrease in plaque size but with less stable plaques, in association with decreased monocyte recruitment. Interestingly, no changes in number of pMos or cMos in blood or BM were noted, although an increased ratio of cMos/pMos was observed in blood. Here, we found increased

pMo numbers in blood, BM, spleen, and aortas and a profound skewing towards pMos within total monocyte populations. Taken together, these studies suggest that LYN is unique within the SFK family as a negative regulator of pMos. This is consistent with its distinction as an important negative regulator of signaling, compared with the other SFKs which more typically act as positive regulators of signal transduction.<sup>46</sup> However, further investigation into the role of other SFKs in regulating pMos and atherosclerosis is needed. Here, we examined how loss of LYN and increased pMo numbers affected the *Ldlr*<sup>-/-</sup> high-fat diet mouse model of atherosclerosis,<sup>73</sup> and found that *Lyn* deficiency in innate immune cells and increased pMo numbers were associated with reduced disease severity. Further studies are required to determine to what extent LYN-mediated changes in pMos versus other innate immune cells play a role in protection against atherosclerosis.

Marcovecchio et al<sup>60</sup> recently showed that recognition of oxLDL by the scavenger receptor CD36 on pMos led to increased patrolling of the vasculature in vivo in an SFK-dependent manner. Interestingly, Lyn has been found to be in complex with CD36 in macrophages and is activated in response to oxLDL. In these studies, CD36 signaling in response to oxLDL was SFK dependent; however, Lyn's specific role in this was unclear.<sup>74,75</sup> In addition, pMos from mice on a high-fat diet have an increase in active SFKs, further supporting a role for SFKs, including LYN, in pMos in atherosclerosis.<sup>60</sup> Here, we showed that loss of LYN increases pMos and aorta-associated pMos. This suggests that LYN negatively regulates pMos and its loss may promote signaling downstream of scavenger receptors such as CD36 leading to increased vascular patrolling. Further studies investigating LYN's role in regulating pMo function and signaling in the context of atherogenic stimuli, such as oxLDL, together with in vivo imaging modalities, should provide further insight into LYN's role in regulating pMo and monocyte-derived macrophages in atherosclerosis.

Interestingly, other studies that have linked pMos to protection from atherosclerosis used Nur77-deficient BM-chimeras or mice, which have a severely impaired pMo compartment.<sup>8,23,24</sup> In these studies, mice lacking Nur77 developed more severe disease, which was linked to an impaired M2, and enhanced M1 macrophage phenotype.<sup>23,24</sup> Within sites of atherogenesis, M1 macrophage responses are thought to contribute to pathological inflammation, whereas M2 responses may be protective.<sup>37,70</sup> *Lyn*<sup>-/-</sup> macrophages are M2 skewed,<sup>76</sup> therefore, loss of LYN in myeloid cells might inhibit atherosclerosis by not only facilitating the expansion of pMos but also by promoting a regulatory macrophage phenotype.

Altered mononuclear phagocyte landscapes are also a feature of human atherosclerosis plaques.<sup>77,78</sup> However, in a human setting, combined genetic polymorphisms

rather than a single mutation (such as *Lyn* total knock-out) are more likely to underlie differences in monocyte biology and atherosclerosis susceptibility/severity. Importantly, loss of a single *Lyn* allele (*Lyn*<sup>+/-</sup>) was sufficient to induce increased pMos in blood, which supports the idea that Lyn-mediated control of pMo populations may have relevance to polygenic human diseases where more subtle changes in Lyn activity/expression and combined regulatory pathway perturbations may impact disease cause. As LYN is expressed in human monocytes and macrophages,<sup>74,79</sup> the data presented here provide a strong rationale for investigating LYN as a potential novel target for treatment of atherosclerosis in humans.

Overall, our data clearly show that key signaling patterns distinguish cMos and pMos and that LYN is a key regulator of pMo homeostasis, signaling, and gene expression with the potential to impact blood vessel-associated disease. Given the recently identified role of pMos in antagonizing lung metastasis<sup>25</sup> it will be interesting to investigate whether loss of LYN, and the associated increase in circulatory pMos, impacts tumour growth or spread. Importantly, kinase inhibitors that target LYN are currently in use in the clinic, and their clinical utility could be expanded for use in diseases where increasing pMo numbers would provide a therapeutic benefit.

## ARTICLE INFORMATION

Received July 17, 2019; revision received March 3, 2020; accepted March 9, 2020.

### Affiliations

From the Department of Microbiology and Immunology (M.E.R., M.B., J.A.F.D.S., R.A.C., W.C., A.W., I.M., K.W.H.), Department of Pediatrics (D.C.T.), Department of Biochemistry and Molecular Biology (S.C., P.R.C.), and Department of Pathology and Laboratory Medicine (J.J.P.), University of British Columbia, Vancouver, Canada; and British Columbia Children's Hospital Research Institute, Vancouver, Canada (D.C.T., J.J.P.).

### Acknowledgments

We thank Dr Danielle Krebs for her insight and editorial input on the article. We also thank the University of British Columbia (UBC) Flow Cytometry Core (Andy Johnson and Justin Wong) and UBC Antibody Lab (Mike Williams) for their contribution to the mass cytometry core and antibody panel generation, respectively. We thank Dr Cheryl Wellington and Emily Button with technical insights into lipid profiling. We thank Jeanette Johnson for critical inputs in the single cell RNA-sequencing data analysis. M.E. Roberts generated majority of the data, performed data analysis, and wrote the first draft of the article. M. Barvalia generated the single cell RNA-sequencing (scRNAseq) data, performed analysis of scRNAseq and mass cytometry data, and contributed to article writing. J.A.F.D. Silva generated data contributing to Figures 6 and 7 and edited the article. R.A. Cederberg contributed to the data in Figures 6 and 7. W. Chu and A. Wong performed flow cytometric analysis of aortic immune cells. D.C. Tai performed aortic dissections and analysis of atherosclerotic plaques. S. Chen and P.R. Cullis provided lipid nanoparticles and associated quality control and expertise. I. Matos assisted with bone marrow radiation chimera studies. J.J. Priatel provided the Nur77<sup>EGFP</sup> mice and edited the article. K.W. Harder conceived of, supervised, and contributed to the writing of the article.

### Sources of Funding

This work was funded by grants to K.W. Harder from the Canadian Institute of Health Research (No. 3367170, No. 298545) and the NanoMedicines Innovation Network (NMNI).

## Disclosures

None.

## Supplemental Materials

Online Supplemental Figure Legends I–VI

Supplementary methods<sup>80–88</sup>

Online Figures I–VI

## REFERENCES

- Jenkins SJ, Hume DA. Homeostasis in the mononuclear phagocyte system. *Trends Immunol.* 2014;35:358–367. doi: 10.1016/j.it.2014.06.006
- Mildner A, Yona S, Jung S. A close encounter of the third kind: monocyte-derived cells. *Adv Immunol.* 2013;120:69–103. doi: 10.1016/B978-0-12-417028-5.00003-X
- Auffray C, Sieweke MH, Geissmann F. Blood monocytes: development, heterogeneity, and relationship with dendritic cells. *Annu Rev Immunol.* 2009;27:669–692. doi: 10.1146/annurev.immunol.021908.132557
- Swirski FK, Nahrendorf M, Etzrodt M, Wildgruber M, Cortez-Retamozo V, Panizzi P, Figueiredo JL, Kohler RH, Chudnovskiy A, Waterman P, et al. Identification of splenic reservoir monocytes and their deployment to inflammatory sites. *Science.* 2009;325:612–616. doi: 10.1126/science.1175202
- Yona S, Kim KW, Wolf Y, Mildner A, Varol D, Breker M, Strauss-Ayali D, Viukov S, Guillemin M, Misharin A, et al. Fate mapping reveals origins and dynamics of monocytes and tissue macrophages under homeostasis. *Immunity.* 2013;38:79–91. doi: 10.1016/j.immuni.2012.12.001
- Jakubczik CV, Randolph GJ, Henson PM. Monocyte differentiation and antigen-presenting functions. *Nat Rev Immunol.* 2017;17:349–362. doi: 10.1038/nri.2017.28
- Geissmann F, Jung S, Littman DR. Blood monocytes consist of two principal subsets with distinct migratory properties. *Immunity.* 2003;19:71–82. doi: 10.1016/s1074-7613(03)00174-2
- Hanna RN, Carlin LM, Hubbeling HG, Nackiewicz D, Green AM, Punt JA, Geissmann F, Hedrick CC. The transcription factor NR4A1 (Nur77) controls bone marrow differentiation and the survival of Ly6C<sup>+</sup> monocytes. *Nat Immunol.* 2011;12:778–785. doi: 10.1038/ni.2063
- Peng Y, Latchman Y, Elkon KB. Ly6C(low) monocytes differentiate into dendritic cells and cross-tolerize T cells through PDL-1. *J Immunol.* 2009;182:2777–2785. doi: 10.4049/jimmunol.0803172
- Menezes S, Melandri D, Anselmi G, Perchet T, Loschko J, Dubrot J, Patel R, Gautier EL, Hugues S, Longhi MP, et al. The heterogeneity of Ly6Chi monocytes controls their differentiation into iNOS<sup>+</sup> macrophages or monocyte-derived dendritic cells. *Immunity.* 2016;45:1205–1218. doi: 10.1016/j.immuni.2016.12.001
- Mildner A, Schönheit J, Giladi A, David E, Lara-Astiaso D, Lorenzo-Vivas E, Paul F, Chappell-Maor L, Priller J, Leutz A, et al. Genomic characterization of murine monocytes reveals C/EBP $\beta$  transcription factor dependence of Ly6C<sup>+</sup> cells. *Immunity.* 2017;46:849–862.e7. doi: 10.1016/j.immuni.2017.04.018
- Thomas GD, Hanna RN, Vasudevan NT, Hamers AA, Romanoski CE, McArdle S, Ross KD, Blatchley A, Yoakum D, Hamilton BA, et al. Deleting an Nr4a1 super-enhancer subdomain ablates Ly6C<sup>low</sup> monocytes while preserving macrophage gene function. *Immunity.* 2016;45:975–987. doi: 10.1016/j.immuni.2016.10.011
- Cros J, Cagnard N, Woollard K, Patey N, Zhang SY, Senechal B, Puel A, Biswas SK, Moshous D, Picard C, et al. Human CD14<sup>dim</sup> monocytes patrol and sense nucleic acids and viruses via TLR7 and TLR8 receptors. *Immunity.* 2010;33:375–386. doi: 10.1016/j.immuni.2010.08.012
- Ingersoll MA, Spanbroek R, Lottaz C, Gautier EL, Frankenberger M, Hoffmann R, Lang R, Haniffa M, Collin M, Tacke F, et al. Comparison of gene expression profiles between human and mouse monocyte subsets. *Blood.* 2010;115:e10–e19. doi: 10.1182/blood-2009-07-235028
- Narni-Mancinelli E, Soudja SM, Crozat K, Dalod M, Gounon P, Geissmann F, Lauvau G. Inflammatory monocytes and neutrophils are licensed to kill during memory responses in vivo. *PLoS Pathog.* 2011;7:e1002457. doi: 10.1371/journal.ppat.1002457
- Robben PM, LaRegina M, Kuziel WA, Sibley LD. Recruitment of Gr-1<sup>+</sup> monocytes is essential for control of acute toxoplasmosis. *J Exp Med.* 2005;201:1761–1769. doi: 10.1084/jem.20050054
- Serbina NV, Salazar-Mather TP, Biron CA, Kuziel WA, Pamer EG. TNF/ iNOS-producing dendritic cells mediate innate immune defense against bacterial infection. *Immunity.* 2003;19:59–70. doi: 10.1016/s1074-7613(03)00171-7



18. Serbina NV, Pamer EG. Monocyte emigration from bone marrow during bacterial infection requires signals mediated by chemokine receptor CCR2. *Nat Immunol*. 2006;7:311–317. doi: 10.1038/ni1309
19. Serbina NV, Kuziel W, Flavell R, Akira S, Rollins B, Pamer EG. Sequential MyD88-independent and -dependent activation of innate immune responses to intracellular bacterial infection. *Immunity*. 2003;19:891–901. doi: 10.1016/s1074-7613(03)00330-3
20. Carlin LM, Stamatides EG, Auffray C, Hanna RN, Glover L, Vizcay-Barrena G, Hedrick CC, Cook HT, Diebold S, Geissmann F. Nr4a1-dependent Ly6C(low) monocytes monitor endothelial cells and orchestrate their disposal. *Cell*. 2013;153:362–375. doi: 10.1016/j.cell.2013.03.010
21. Michaud JP, Bellavance MA, Préfontaine P, Rivest S. Real-time in vivo imaging reveals the ability of monocytes to clear vascular amyloid beta. *Cell Rep*. 2013;5:646–653. doi: 10.1016/j.celrep.2013.10.010
22. Auffray C, Fogg D, Garfa M, Elain G, Join-Lambert O, Kayal S, Sarnacki S, Cumano A, Lauvaud G, Geissmann F. Monitoring of blood vessels and tissues by a population of monocytes with patrolling behavior. *Science*. 2007;317:666–670. doi: 10.1126/science.1142883
23. Hanna RN, Shaked I, Hubbeling HG, Punt JA, Wu R, Herrley E, Zaugg C, Pei H, Geissmann F, Ley K, et al. NR4A1 (Nur77) deletion polarizes macrophages toward an inflammatory phenotype and increases atherosclerosis. *Circ Res*. 2012;110:416–427. doi: 10.1161/CIRCRESAHA.111.253377
24. Hamers AA, Vos M, Rassam F, Marinković G, Marincovic G, Kurakula K, van Gorp PJ, de Winther MP, Gijbels MJ, de Waard V, et al. Bone marrow-specific deficiency of nuclear receptor Nur77 enhances atherosclerosis. *Circ Res*. 2012;110:428–438. doi: 10.1161/CIRCRESAHA.111.260760
25. Hanna RN, Cekic C, Sag D, Tacke R, Thomas GD, Nowyhed H, Herrley E, Rasquinha N, McArdle S, Wu R, et al. Patrolling monocytes control tumor metastasis to the lung. *Science*. 2015;350:985–990. doi: 10.1126/science.aac9407
26. Plebanek MP, Angeloni NL, Vinokour E, Li J, Henkin A, Martinez-Marin D, Filleur S, Bhowmick R, Henkin J, Miller SD, et al. Pre-metastatic cancer exosomes induce immune surveillance by patrolling monocytes at the metastatic niche. *Nat Commun*. 2017;8:1319. doi: 10.1038/s41467-017-01433-3
27. Romano E, Kusio-Kobialka M, Foukas PG, Baumgaertner P, Meyer C, Ballabeni P, Michielin O, Weide B, Romero P, Speiser DE. Ipilimumab-dependent cell-mediated cytotoxicity of regulatory T cells ex vivo by nonclassical monocytes in melanoma patients. *Proc Natl Acad Sci U S A*. 2015;112:6140–6145. doi: 10.1073/pnas.1417320112
28. Misharin AV, Cuda CM, Saber R, Turner JD, Gierut AK, Haines GK 3<sup>rd</sup>, Berdnikovs S, Filer A, Clark AR, Buckley CD, et al. Nonclassical Ly6C(+) monocytes drive the development of inflammatory arthritis in mice. *Cell Rep*. 2014;9:591–604. doi: 10.1016/j.celrep.2014.09.032
29. Amano H, Amano E, Santiago-Raber ML, Moll T, Martinez-Soria E, Fossati-Jimack L, Iwamoto M, Rozzo SJ, Kotzin BL, Izui S. Selective expansion of a monocyte subset expressing the CD11c dendritic cell marker in the yaa model of systemic lupus erythematosus. *Arthritis Rheum*. 2005;52:2790–2798. doi: 10.1002/art.21365
30. Santiago-Raber ML, Amano H, Amano E, Baudino L, Otani M, Lin Q, Nimmerjahn F, Verbeek JS, Ravetch JV, Takasaki Y, et al. Fcγ receptor-dependent expansion of a hyperactive monocyte subset in lupus-prone mice. *Arthritis Rheum*. 2009;60:2408–2417. doi: 10.1002/art.24787
31. Kuriakose J, Redecke V, Guy C, Zhou J, Wu R, Ippagunta SK, Tillman H, Walker PD, Vogel P, Häcker H. Patrolling monocytes promote the pathogenesis of early lupus-like glomerulonephritis. *J Clin Invest*. 2019;129:2251–2265. doi: 10.1172/JCI125116
32. Jung K, Heishi T, Khan OF, Kowalski PS, Incio J, Rahbari NN, Chung E, Clark JW, Willett CG, Luster AD, et al. Ly6Clo monocytes drive immunosuppression and confer resistance to anti-VEGFR2 cancer therapy. *J Clin Invest*. 2017;127:3039–3051. doi: 10.1172/JCI93182
33. Tamura A, Hirai H, Yokota A, Kamio N, Sato A, Shoji T, Kashiwagi T, Torikoshi Y, Miura Y, Tenen DG, et al. C/EBPβ is required for survival of Ly6C- monocytes. *Blood*. 2017;130:1809–1818. doi: 10.1182/blood-2017-03-772962
34. Landsman L, Bar-On L, Zernecke A, Kim KW, Krauthgamer R, Shagdarsuren E, Lira SA, Weissman IL, Weber C, Jung S. CX3CR1 is required for monocyte homeostasis and atherogenesis by promoting cell survival. *Blood*. 2009;113:963–972. doi: 10.1182/blood-2008-07-170787
35. Debien E, Mayol K, Bjaouk V, Daussy C, De Agüero MG, Taillardet M, Dagany N, Brinza L, Henry T, Dubois B, et al. S1PR5 is pivotal for the homeostasis of patrolling monocytes. *Eur J Immunol*. 2013;43:1667–1675. doi: 10.1002/eji.201343312
36. Lewis ND, Haxhinasto SA, Anderson SM, Stefanopoulos DE, Fogal SE, Adusumalli P, Desai SN, Patnaude LA, Lukas SM, Ryan KR, et al. Circulating monocytes are reduced by sphingosine-1-phosphate receptor modulators independently of S1P3. *J Immunol*. 2013;190:3533–3540. doi: 10.4049/jimmunol.1201810
37. Moore KJ, Sheedy FJ, Fisher EA. Macrophages in atherosclerosis: a dynamic balance. *Nat Rev Immunol*. 2013;13:709–721. doi: 10.1038/nri3520
38. Hilgendorf I, Swirski FK, Robbins CS. Monocyte fate in atherosclerosis. *Arterioscler Thromb Vasc Biol*. 2015;35:272–279. doi: 10.1161/ATVBAHA.114.303565
39. Tabas I, Lichtman AH. Monocyte-macrophages and T cells in atherosclerosis. *Immunity*. 2017;47:621–634. doi: 10.1016/j.immuni.2017.09.008
40. Wu H, Perrard XD, Wang Q, Perrard JL, Polsani VR, Jones PH, Smith CW, Ballantyne CM. CD11c expression in adipose tissue and blood and its role in diet-induced obesity. *Arterioscler Thromb Vasc Biol*. 2010;30:186–192. doi: 10.1161/ATVBAHA.109.198044
41. Bishop JL, Roberts ME, Beer JL, Huang M, Chehal MK, Fan X, Fouser LA, Ma HL, Bacani JT, Harder KW. Lyn activity protects mice from DSS colitis and regulates the production of SC family from innate lymphoid cells. *Mucosal Immunol*. 2014;7:405–416. doi: 10.1038/mi.2013.60
42. Ingley E. Functions of the Lyn tyrosine kinase in health and disease. *Cell Commun Signal*. 2012;10:21. doi: 10.1186/1478-811X-10-21
43. Tsukita S, Oishi K, Akiyama T, Yamanashi Y, Yamamoto T, Tsukita S. Specific proto-oncogenic tyrosine kinases of Src family are enriched in cell-to-cell adherens junctions where the level of tyrosine phosphorylation is elevated. *J Cell Biol*. 1991;113:867–879. doi: 10.1083/jcb.113.4.867
44. Ikeda K, Nakayama Y, Togashi Y, Obata Y, Kuga T, Kasahara K, Fukumoto Y, Yamaguchi N. Nuclear localization of Lyn tyrosine kinase mediated by inhibition of its kinase activity. *Exp Cell Res*. 2008;314:3392–3404. doi: 10.1016/j.yexcr.2008.08.019
45. Siyanova EY, Serfas MS, Mazo IA, Tyner AL. Tyrosine kinase gene expression in the mouse small intestine. *Oncogene*. 1994;9:2053–2057.
46. Scapini P, Pereira S, Zhang H, Lowell CA. Multiple roles of Lyn kinase in myeloid cell signaling and function. *Immunol Rev*. 2009;228:23–40. doi: 10.1111/j.1600-065X.2008.00758.x
47. Harder KW, Parsons LM, Armes J, Evans N, Kountouri N, Clark R, Quilici C, Grail D, Hodgson GS, Dunn AR, et al. Gain- and loss-of-function Lyn mutant mice define a critical inhibitory role for Lyn in the myeloid lineage. *Immunity*. 2001;15:603–615. doi: 10.1016/s1074-7613(01)00208-4
48. Harder KW, Quilici C, Naik E, Inglesse M, Kountouri N, Turner A, Zlatić K, Tarlinton DM, Hibbs ML. Perturbed myeloerythropoiesis in Lyn-deficient mice is similar to that in mice lacking the inhibitory phosphatases SHP-1 and SHP-1. *Blood*. 2004;104:3901–3910. doi: 10.1182/blood-2003-12-4396
49. Scapini P, Hu Y, Chu CL, Migone TS, Defranco AL, Cassatella MA, Lowell CA. Myeloid cells, BAFF, and IFN-γ establish an inflammatory loop that exacerbates autoimmunity in Lyn-deficient mice. *J Exp Med*. 2010;207:1757–1773. doi: 10.1084/jem.20100086
50. Amir el-AD, Davis KL, Tadmor MD, Simonds EF, Levine JH, Bendall SC, Shenfeld DK, Krishnaswamy S, Nolan GP, Pe'er D. viSNE enables visualization of high dimensional single-cell data and reveals phenotypic heterogeneity of leukemia. *Nat Biotechnol*. 2013;31:545–552. doi: 10.1038/nbt.2594
51. Hibbs ML, Tarlinton DM, Armes J, Grail D, Hodgson G, Maglitt R, Stacker SA, Dunn AR. Multiple defects in the immune system of Lyn-deficient mice, culminating in autoimmune disease. *Cell*. 1995;83:301–311. doi: 10.1016/0092-8674(95)90171-x
52. Mombaerts P, Iacomini J, Johnson RS, Herrup K, Tonegawa S, Papaioannou VE. RAG-1-deficient mice have no mature B and T lymphocytes. *Cell*. 1992;68:869–877. doi: 10.1016/0092-8674(92)90030-g
53. Shekhar K, Brodin P, Davis MM, Chakraborty AK. Automatic Classification of Cellular Expression by Nonlinear Stochastic Embedding (ACCENSE). *Proc Natl Acad Sci U S A*. 2014;111:202–207. doi: 10.1073/pnas.1321405111
54. Akagi T, Thoenissen NH, George A, Crooks G, Song JH, Okamoto R, Nowak D, Gombart AF, Koeffler HP. In vivo deficiency of both C/EBPβ and C/EBPε results in highly defective myeloid differentiation and lack of cytokine response. *PLoS One*. 2010;5:e15419. doi: 10.1371/journal.pone.0015419
55. Endoh Y, Chung YM, Clark IA, Geczy CL, Hsu K. IL-10-dependent S100A8 gene induction in monocytes/macrophages by double-stranded RNA. *J Immunol*. 2009;182:2258–2268. doi: 10.4049/jimmunol.0802683
56. Gery S, Gombart AF, Yi WS, Koeffler C, Hofmann WK, Koeffler HP. Transcription profiling of C/EBP targets identifies Per2 as a gene implicated in myeloid leukemia. *Blood*. 2005;106:2827–2836. doi: 10.1182/blood-2005-01-0358
57. Baran CP, Tridandapani S, Helgason CD, Humphries RK, Krystal G, Marsh CB. The inositol 5'-phosphatase SHIP-1 and the Src kinase Lyn negatively regulate macrophage colony-stimulating factor-induced Akt activity. *J Biol Chem*. 2003;278:38628–38636. doi: 10.1074/jbc.M305021200

58. Rohde CM, Schrum J, Lee AW. A juxtamembrane tyrosine in the colony stimulating factor-1 receptor regulates ligand-induced Src association, receptor kinase function, and down-regulation. *J Biol Chem*. 2004;279:43448–43461. doi: 10.1074/jbc.M314170200
59. Patel AA, Zhang Y, Fullerton JN, Boelen L, Rongvaux A, Maini AA, Bigley V, Flavell RA, Gilroy DW, Asquith B, et al. The fate and lifespan of human monocyte subsets in steady state and systemic inflammation. *J Exp Med*. 2017;214:1913–1923. doi: 10.1084/jem.20170355
60. Marcovecchio PM, Thomas GD, Mikulski Z, Ehinger E, Mueller KAL, Blatchley A, Wu R, Miller YI, Nguyen AT, Taylor AM, et al. Scavenger receptor CD36 directs nonclassical monocyte patrolling along the endothelium during early atherogenesis. *Arterioscler Thromb Vasc Biol*. 2017;37:2043–2052. doi: 10.1161/ATVBAHA.117.309123
61. Ishibashi S, Brown MS, Goldstein JL, Gerard RD, Hammer RE, Herz J. Hypercholesterolemia in low density lipoprotein receptor knockout mice and its reversal by adenovirus-mediated gene delivery. *J Clin Invest*. 1993;92:883–893. doi: 10.1172/JCI116663
62. Bosco N, Sweet LK, Bénard A, Ceredig R, Rolink A. Auto-reconstitution of the T-cell compartment by radioresistant hematopoietic cells following lethal irradiation and bone marrow transplantation. *Exp Hematol*. 2010;38:222–232.e2. doi: 10.1016/j.exphem.2009.12.006
63. Anderson BE, McNiff JM, Matte C, Athanasiadis I, Shlomchik WD, Shlomchik MJ. Recipient CD4+ T cells that survive irradiation regulate chronic graft-versus-host disease. *Blood*. 2004;104:1565–1573. doi: 10.1182/blood-2004-01-0328
64. Komatsu N, Hori S. Full restoration of peripheral Foxp3+ regulatory T cell pool by radioresistant host cells in scurfy bone marrow chimeras. *Proc Natl Acad Sci U S A*. 2007;104:8959–8964. doi: 10.1073/pnas.0702004104
65. Tsantikos E, Maxwell MJ, Putoczki T, Ernst M, Rose-John S, Tarlinton DM, Hibbs ML. Interleukin-6 trans-signaling exacerbates inflammation and renal pathology in lupus-prone mice. *Arthritis Rheum*. 2013;65:2691–2702. doi: 10.1002/art.38061
66. Tsantikos E, Oracki SA, Quilici C, Anderson GP, Tarlinton DM, Hibbs ML. Autoimmune disease in Lyn-deficient mice is dependent on an inflammatory environment established by IL-6. *J Immunol*. 2010;184:1348–1360. doi: 10.4049/jimmunol.0901878
67. MacDonald KP, Palmer JS, Cronau S, Seppanen E, Olver S, Raffelt NC, Kuns R, Pettit AR, Clouston A, Wainwright B, et al. An antibody against the colony-stimulating factor 1 receptor depletes the resident subset of monocytes and tissue- and tumor-associated macrophages but does not inhibit inflammation. *Blood*. 2010;116:3955–3963. doi: 10.1182/blood-2010-02-266296
68. Wiktor-Jedrzejczak W, Ratajczak MZ, Ptasznik A, Sell KW, Ahmed-Ansari A, Ostertag W. CSF-1 deficiency in the op/op mouse has differential effects on macrophage populations and differentiation stages. *Exp Hematol*. 1992;20:1004–1010.
69. Dai XM, Ryan GR, Hapel AJ, Dominguez MG, Russell RG, Kapp S, Sylvestre V, Stanley ER. Targeted disruption of the mouse colony-stimulating factor 1 receptor gene results in osteopetrosis, mononuclear phagocyte deficiency, increased primitive progenitor cell frequencies, and reproductive defects. *Blood*. 2002;99:111–120. doi: 10.1182/blood.v99.1.111
70. Ley K, Miller YI, Hedrick CC. Monocyte and macrophage dynamics during atherogenesis. *Arterioscler Thromb Vasc Biol*. 2011;31:1506–1516. doi: 10.1161/ATVBAHA.110.221127
71. Lowell CA. Src-family kinases: rheostats of immune cell signaling. *Mol Immunol*. 2004;41:631–643. doi: 10.1016/j.molimm.2004.04.010
72. Medina I, Cougoule C, Drechsler M, Bermudez B, Koenen RR, Sluimer J, Wolfs I, Döring Y, Herias V, Gijbels M, et al. Hck/Fgr kinase deficiency reduces plaque growth and stability by blunting monocyte recruitment and intraplaque motility. *Circulation*. 2015;132:490–501. doi: 10.1161/CIRCULATIONAHA.114.012316
73. Ishibashi S, Goldstein JL, Brown MS, Herz J, Burns DK. Massive xanthomatosis and atherosclerosis in cholesterol-fed low density lipoprotein receptor-negative mice. *J Clin Invest*. 1994;93:1885–1893. doi: 10.1172/JCI117179
74. Chen Y, Kennedy DJ, Ramakrishnan DP, Yang M, Huang W, Li Z, Xie Z, Chadwick AC, Sahoo D, Silverstein RL. Oxidized LDL-bound CD36 recruits an Na<sup>+</sup>/K<sup>+</sup>-ATPase-Lyn complex in macrophages that promotes atherosclerosis. *Sci Signal*. 2015;8:ra91. doi: 10.1126/scisignal.aaa9623
75. Rahaman SO, Lennon DJ, Febbraio M, Podrez EA, Hazen SL, Silverstein RL. A CD36-dependent signaling cascade is necessary for macrophage foam cell formation. *Cell Metab*. 2006;4:211–221. doi: 10.1016/j.cmet.2006.06.007
76. Xiao W, Hong H, Kawakami Y, Lowell CA, Kawakami T. Regulation of myeloproliferation and M2 macrophage programming in mice by Lyn/Hck, SHIP, and Stat5. *J Clin Invest*. 2008;118:924–934. doi: 10.1172/JCI34013
77. Winkels H, Ehinger E, Vassallo M, Buscher K, Dinh HQ, Kobiyama K, Hamers AAJ, Cochain C, Vafadarnejad E, Saliba AE, et al. Atlas of the immune cell repertoire in mouse atherosclerosis defined by single-cell RNA-sequencing and mass cytometry. *Circ Res*. 2018;122:1675–1688. doi: 10.1161/CIRCRESAHA.117.312513
78. Cochain C, Vafadarnejad E, Arampatzis P, Pelisek J, Winkels H, Ley K, Wolf D, Saliba AE, Zernecke A. Single-cell RNA-seq reveals the transcriptional landscape and heterogeneity of aortic macrophages in murine atherosclerosis. *Circ Res*. 2018;122:1661–1674. doi: 10.1161/CIRCRESAHA.117.312509
79. Wang AV, Scholl PR, Geha RS. Physical and functional association of the high affinity immunoglobulin G receptor (Fc gamma RI) with the kinases Hck and Lyn. *J Exp Med*. 1994;180:1165–1170. doi: 10.1084/jem.180.3.1165
80. Krebs DL, Chehal MK, Sio A, Huntington ND, Da ML, Ziltener P, Inglese M, Kountouri N, Priatel JJ, Jones J, et al. Lyn-dependent signaling regulates the innate immune response by controlling dendritic cell activation of NK cells. *J Immunol*. 2012;188:5094–5105. doi: 10.4049/jimmunol.1103395
81. Moran AE, Holzapfel KL, Xing Y, Cunningham NR, Maltzman JS, Punt J, Hogquist KA. T cell receptor signal strength in Treg and iNKT cell development demonstrated by a novel fluorescent reporter mouse. *J Exp Med*. 2011;208:1279–1289. doi: 10.1084/jem.20110308
82. Stuart T, Butler A, Hoffman P, Hafemeister C, Papalexi E, Mauck WM 3<sup>rd</sup>, Hao Y, Stoeckius M, Smibert P, Satija R. Comprehensive integration of single-cell data. *Cell*. 2019;177:1888–1902.e21. doi: 10.1016/j.cell.2019.05.031
83. Butler A, Hoffman P, Smibert P, Papalexi E, Satija R. Integrating single-cell transcriptomic data across different conditions, technologies, and species. *Nat Biotechnol*. 2018;36:411–420. doi: 10.1038/nbt.4096
84. McGinnis CS, Murrow LM, Gartner ZJ. DoubletFinder: doublet detection in single-cell RNA sequencing data using artificial nearest neighbors. *Cell Syst*. 2019;8:329–337.e4. doi: 10.1016/j.cels.2019.03.003
85. Chen S, Tam YY, Lin PJ, Leung AK, Tam YK, Cullis PR. Development of lipid nanoparticle formulations of siRNA for hepatocyte gene silencing following subcutaneous administration. *J Control Release*. 2014;196:106–112. doi: 10.1016/j.jconrel.2014.09.025
86. Akinc A, Zumbuehl A, Goldberg M, Leshchiner ES, Busini V, Hossain N, Bacallado SA, Nguyen DN, Fuller J, Alvarez R, et al. A combinatorial library of lipid-like materials for delivery of RNAi therapeutics. *Nat Biotechnol*. 2008;26:561–569. doi: 10.1038/nbt1402
87. Montesano R, Pepper MS, Möhle-Steinlein U, Risau W, Wagner EF, Orci L. Increased proteolytic activity is responsible for the aberrant morphogenetic behavior of endothelial cells expressing the middle T oncogene. *Cell*. 1990;62:435–445. doi: 10.1016/0092-8674(90)90009-4
88. Schindelin J, Arganda-Carreras I, Frise E, Kaynig V, Longair M, Pietzsch T, Preibisch S, Rueden C, Saalfeld S, Schmid B, et al. Fiji: an open-source platform for biological-image analysis. *Nat Methods*. 2012;9:676–682. doi: 10.1038/nmeth.2019